Identifying Long-Run Risks: A Bayesian Mixed-Frequency Approach

Frank Schorfheide*
University of Pennsylvania
CEPR and NBER

Dongho Song
Boston College

Amir Yaron
University of Pennsylvania
NBER

This Version: April 11, 2016

Abstract

We develop a novel state-space model that identifies both a persistent conditional mean and a time-varying volatility component in consumption growth. We utilize a mixed-frequency approach that allows us to augment post-1959 monthly data with annual observations dating back to 1930. The use of monthly data is important for identifying the stochastic volatility process; yet the data are contaminated, which makes the inclusion of measurement errors essential for identifying the predictable component. Once dividend growth and asset return data are included in the estimation, we find even stronger evidence for the persistent component. The estimated cash flow dynamics in conjunction with recursive preferences generate asset prices in an endowment economy that are largely consistent with the data. The model with asset prices identifies three volatility processes. The one for the predictable cash flow component is crucial for asset pricing, whereas the other two are important for tracking the data. To estimate this model we use a particle MCMC approach that exploits the conditional linear structure of the approximate equilibrium in the endowment economy.

*Correspondence: Department of Economics, 3718 Locust Walk, University of Pennsylvania, Philadelphia, PA 19104-6297. Email: schorf@ssc.upenn.edu (Frank Schorfheide). Department of Economics, Boston College, 140 Commonwealth Avenue, Chestnut Hill, MA 02467. Email: dongho.song@bc.edu (Dongho Song). The Wharton School, University of Pennsylvania, Philadelphia, PA 19104-6367. Email: yaron@wharton.upenn.edu (Amir Yaron).
We thank Bent J. Christensen, Ian Dew-Becker, Frank Diebold, Emily Fox, Roberto Gomez Cram, Lars Hansen, Arthur Lewbel, Lars Lochstoer, Ivan Shaliastovich, Neil Shephard, Minchul Shin, and seminar participants at the 2013 SED Meeting, the 2013 SBIES Meeting, the 2014 AEA Meeting, the 2014 Aarhus Macro-Finance Symposium, the 2015 UBC Summer Finance Conference, the 2016 AFA Meeting, the Board of Governors, Boston College, Boston University, Columbia University, Cornell University, the European Central Bank, Indiana University, Ohio State University, Tel Aviv University, Universite de Toulouse, University of Illinois, and University of Pennsylvania for helpful comments and discussions. Schorfheide gratefully acknowledges financial support from the National Science Foundation under Grant SES 1061725. Yaron thanks the Rodney White Center for financial support.

1 Introduction

The dynamics of aggregate consumption play a key role in business cycle models, tests of the permanent income hypothesis, and asset pricing. Perhaps surprisingly, there is a significant disagreement about the basic time series properties of consumption. First, while part of the profession holds a long-standing view that aggregate consumption follows a random walk and its growth rates are serially uncorrelated, e.g., Hall (1978) and Campbell and Cochrane (1999), the recent literature on long-run risks (LRR), e.g., Bansal and Yaron (2004) and Hansen, Heaton, and Li (2008), emphasizes the presence of a small persistent component in consumption growth.[1] Second, while time-varying volatility was a feature that until recently was mainly associated with financial time series, there is now a rapidly growing literature stressing the importance of stochastic volatility in macroeconomic aggregates, e.g., Bansal and Yaron (2004), Bloom (2009), and Fernández-Villaverde and Rubio-Ramírez (2011), and the occurrence of rare disasters, e.g., Barro (2009) and Gourio (2012).

Studying consumption growth dynamics leads to the following challenge. On the one hand, it is difficult to identify the time-varying volatility based on time-aggregated data, e.g., Drost and Nijman (1993), which favors the use of high-frequency monthly data. On the other hand, monthly consumption growth data are contaminated by measurement error, e.g., Slesnick (1998) and Wilcox (1992), which mask the dynamics of the underlying process. We address this challenge by developing a novel Bayesian state-space model with a measurement error component that allows us to identify both a persistent component of consumption growth as well as its time-varying volatility. The model is tailored toward monthly data, but a mixed-frequency approach allows us to accommodate annual consumption growth data up to the Great Depression era.

When the dynamics of consumption growth are estimated jointly with dividend growth data and asset returns, we find even stronger evidence (tighter credible intervals) for the persistent component and are able to identify three separate volatility components: one governing dynamics of the persistent cash flow growth component, and the other two controlling temporally independent shocks to consumption and dividend volatility. We show that these consumption and dividend dynamics in conjunction with recursive preferences with early resolution of uncertainty generate asset prices in a representative agent endowment economy that are largely consistent with the data. The stochastic volatility process for the persistent component is important for asset prices, while the other two volatility processes only have a small impact on asset prices but are important for tracking the data.

[1] The literature on robustness, e.g., Hansen and Sargent (2007), highlights that merely contemplating low-frequency shifts in consumption growth can be important for macroeconomic outcomes and asset prices.

The first part of our empirical analysis starts with the estimation of a state-space model according to which consumption growth is the sum of an *iid* and an AR(1) component, focusing on the persistence ρ of the AR(1) component. We show that once we include monthly measurement errors that average out at the annual frequency, the fit of the model improves significantly, and we obtain an estimate of ρ around 0.92.[2] While according to our estimates more than half of the variation in monthly consumption growth is due to measurement errors, we verify that the estimation of the monthly model with measurement errors leads to a more accurate estimate of ρ than the estimation with time-aggregated data. Importantly, adding stochastic volatility leads to a further improvement in model fit, a reduction in the posterior uncertainty about ρ, and an increase in the point estimate of ρ to 0.95. Next, we augment the state-space model to include a measurement equation for dividend growth. The joint estimation based on consumption and dividend growth based on post-1959 data leads to a ρ of 0.97. The point estimate falls slightly if the sample is extended to the Great Depression era.

The second part of the empirical analysis examines the economic implications of the estimated consumption and dividend growth processes by embedding them into an representative agent endowment economy as in Bansal and Yaron (2004). This model is referred to as long run risks (LRR) model. Our model distinguishes itself from the existing LRR literature in several important dimensions. First, as previously discussed, our model for the cash flows includes measurement errors and three volatility processes to improve the fit. Second, we specify an additional process for variation in the time rate of preference as in Albuquerque, Eichenbaum, Luo, and Rebelo (2016), which generates risk-free rate variation that is independent of cash flows and leads to an improved fit for the risk-free rate.

To incorporate market returns and the risk-free rate into our state-space model we solve for the asset pricing implications of the LRR model to obtain measurement equations for these two series.[3] Bayesian inference in the model with asset prices is considerably more difficult than in the cash-flow-only specification and requires the following technical innovation. The posterior sampler requires us to evaluate the likelihood function of our state-space model with a nonlinear filter. Due to the high-dimensional state space that arises from the mixed-frequency setting, this nonlinear filtering is a seemingly daunting task. We show how to exploit the partially linear structure of the state-space model to derive a very efficient sequential Monte Carlo (particle) filter. Unlike the

[2]Without accounting for measurement errors, the estimate of ρ using monthly consumption growth data is insignificantly different from 0 which can partly account for some view that consumption growth is an *iid* process.

[3]In order to solve the model, we approximate the exponential Gaussian volatility processes by linear Gaussian processes such that the standard analytical solution techniques that have been widely used in the LRR literature can be applied. The approximation of the exponential volatility process is used only to derive the coefficients in the law of motion of the asset prices.

generalized method of moments (GMM) approach that is common in the long-run-risks literature, our sophisticated state-space approach lets us track the predictable component x_t as well as the stochastic volatilities over time. In turn, this allows us to construct period-by-period decompositions of risk premia and asset price variances.

The estimation of the LRR model delivers the following important empirical findings. First, the estimate of ρ, i.e., the autocorrelation of the persistent cash flow component, is 0.987, somewhat higher than what we obtained based on the cash-flow-only estimation. Importantly, we show that the time path of the persistent component looks very similar with and without asset price data. Second, as we previously mentioned, all three stochastic volatility processes display significant time variation yet behave distinctly over time. The volatility processes partly capture heteroskedasticity of innovations, and in part they break some of the tight links that the model imposes on the conditional mean dynamics of asset prices and cash flows. This feature significantly improves the model implications for consumption and return predictability. As emphasized by the LRR literature, the volatility processes have to be very persistent in order to have significant quantitative effects on asset prices.

An important feature of our estimation is that the likelihood focuses on conditional correlations between the risk-free rate and consumption — a dimension often not directly targeted in the literature. We show that because consumption growth and its volatility determine the risk-free rate dynamics, one requires another independent volatility process to account for the weak correlation between consumption growth and the risk-free rate. The independent time rate of preference shocks mute the model-implied correlation further and improve the model fit in regard to the risk-free rate dynamics.

Third, it is worth noting that the median posterior estimate for risk aversion is 8-9 while it is around 1.9 for the intertemporal elasticity of substitution (IES). These estimates are broadly consistent with the parameter values highlighted in the LRR literature (see Bansal, Kiku, and Yaron (2012), and Bansal, Kiku, and Yaron (2014)). Fourth, at the estimated preference parameters and those characterizing the consumption and dividend dynamics, the model is able to successfully generate many key asset-pricing moments, and improve model performance relative to previous LRR models along several dimensions.[4] In particular, the posterior median of the equity premium is 8%, while the model's posterior predictive distribution is consistent with the observed large volatility of the price-dividend ratio at 0.45, and the R^2s from predicting returns and consumption growth by the price-dividend ratio.

[4] It is worth noting that the model is able to generate reasonable asset pricing implications even when it is estimated based only on cash flow data.

Our paper is connected to several strands of the literature. In terms of the LRR literature, Bansal, Kiku, and Yaron (2014) utilize data that are time-aggregated to annual frequency to estimate the LRR model by GMM and Bansal, Gallant, and Tauchen (2007) pursue an approach based on the efficient method of moments (EMM). Both papers use cash flow *and* asset price data jointly for the estimation of the parameters of the cash flow process. Our likelihood-based approach provides evidence which is broadly consistent with the results highlighted in those paper and other calibrated LRR models, e.g., Bansal, Kiku, and Yaron (2012). Our likelihood function implicitly utilizes a broader set of moments than earlier GMM or EMM estimation approaches. These moments include the entire sequence of autocovariances as well as higher-order moments of the time series used in the estimation and let us measure the time path of the predictable component of cash flows as well as the time path of the innovation volatilities. Rather than asking the model to fit a few selected moments, we are raising the bar and force the model to track cash flow and asset return time series. Finally, it is worth noting that our paper distinguishes itself from previous LRR literature in showing that even by just using monthly consumption growth data with an appropriate measurement error structure, we are able to estimate the highly persistent predictable component. In complimentary research Nakamura, Sergeyev, and Steinsson (2015) show that an estimation based on a long cross-country panel of annual consumption data also yields large estimates of the autocorrelation of the persistent component.

To implement Bayesian inference, we embed a particle-filter-based likelihood approximation into a Metropolis-Hastings algorithm as in Fernández-Villaverde and Rubio-Ramírez (2007) and Andrieu, Doucet, and Holenstein (2010). This algorithm belongs to the class of particle Markov chain Monte Carlo (MCMC) algorithms. Because our state-space system is linear conditional on the volatility states, we can use Kalman-filter updating to integrate out a subset of the state variables. The genesis of this idea appears in the mixture Kalman filter of Chen and Liu (2000). Particle filter methods are also utilized in Johannes, Lochstoer, and Mou (2016), who estimate an asset pricing model in which agents have to learn about the parameters of the cash flow process from consumption growth data. While Johannes, Lochstoer, and Mou (2016) examine the role of parameter uncertainty for asset prices, which is ignored in our analysis, they use a more restrictive version of the cash flow process and do not utilize mixed-frequency observations.[5]

Our state-space setup makes it relatively straightforward to utilize data that are available at different frequencies. The use of state-space systems to account for missing monthly observations dates back to at least Harvey (1989) and has more recently been used in the context of dynamic

[5]Building on our approach, Creal and Wu (2015) use gamma processes to model time-varying volatilities and estimate a yield curve model using particle MCMC. Doh and Wu (2015) estimate a nonlinear asset pricing model in which all the asset prices and the consumption process are quadratic rather than linear function of the states.

factor models (see, e.g., Mariano and Murasawa (2003) and Aruoba, Diebold, and Scotti (2009)) and VARs (see, e.g., Schorfheide and Song (2015)). Finally, there is a growing and voluminous literature in macro and finance that highlights the importance of volatility for understanding the macroeconomy and financial markets (see, e.g., Bansal, Khatacharian, and Yaron (2005), Bloom (2009), Fernández-Villaverde and Rubio-Ramírez (2011), Bansal, Kiku, and Yaron (2012), and Bansal, Kiku, Shaliastovich, and Yaron (2014)). Our volatility specification that accommodates three processes further contributes to identifying the different uncertainty shocks in the economy.

The remainder of the paper is organized as follows. Section 2 describes the measurement error models for consumption and dividend growth, the data set, and Bayesian inference for the cash-flow-only estimation. Section 3 presents the empirical findings based on the consumption and dividend growth data. Section 4 introduces the LRR model environment, describes the model solution and the particle MCMC approach used to implement Bayesian inference. Section 5 discusses the empirical findings obtained from the estimation of the LRR model and Section 6 provides concluding remarks.

2 Modeling Consumption and Dividend Growth

The first step of our analysis is to develop an empirical state-space model for consumption and dividend growth, focusing mostly on the measurement equations of the state-space model. We take the length of the period to be one month. The use of monthly data is important for identifying stochastic volatility processes. Unfortunately, consumption data are less accurate at monthly frequency than at the more widely-used quarterly or annual frequencies. In this regard, the main contribution in this section is a novel specification of a measurement error model for consumption growth, which has the feature that monthly measurement errors average out under temporal aggregation. While dividend data are available at monthly frequency from 1930 onwards, monthly consumption data have only been published since 1959. Thus, we adapt the measurement equation to the data availability.

In terms of notation, we will distinguish between observed consumption and dividend growth, denoted by $g^o_{c,t}$ and $g^o_{d,t}$, from "true" (or model-implied) consumption and dividend growth, denoted by $g_{c,t}$ and $g_{d,t}$. The measurement equations for observed consumption and dividend growth are developed in Sections 2.1 and 2.2, respectively. We provide a brief discussion of the data used in the empirical analysis in Section 2.3. We present a benchmark state-transition equation in Section 2.4 and summarize the Bayesian techniques used to estimate the cash flow model.

2.1 A Measurement Equation for Consumption

In our empirical analysis we use annual consumption growth rates prior to 1959 and monthly consumption growth rates subsequently.[6] The measurement equation for consumption in our state-space representation has to be general enough to capture two features: (i) the switch from annual to monthly observations in 1959, and (ii) measurement errors that are potentially larger at a monthly frequency than an annual frequency. To describe the measurement equation for consumption growth data, we introduce some additional notation. We use C_t^o and C_t to denote the observed and the "true" level of consumption, respectively. Moreover, we represent the monthly time subscript t as $t = 12(j-1)+m$, where $m = 1, \ldots, 12$. Here j indexes the year and m the month within the year. We proceed in two steps. First, we derive a measurement equation for consumption growth at the annual frequency, which is used for pre-1959 data. Second, we specify a measurement equation for consumption growth at the monthly frequency, which is used for post-1959 data.

Measurement of Annual Consumption Growth. We define annual consumption as the sum of monthly consumption over the span of one year, i.e.:

$$C_{(j)}^a = \sum_{m=1}^{12} C_{12(j-1)+m}.$$

Log-linearizing this relationship around a monthly value C_* and defining lowercase c as percentage deviations from the log-linearization point, i.e., $c = \log C/C_*$, we obtain

$$c_{(j)}^a = \frac{1}{12}\sum_{m=1}^{12} c_{12(j-1)+m}.$$

Thus, monthly consumption growth rates can be defined as

$$g_{c,t} = c_t - c_{t-1}$$

and annual growth rates are given by

$$g_{c,(j)}^a = c_{(j)}^a - c_{(j-1)}^a = \sum_{\tau=1}^{23}\left(\frac{12-|\tau-12|}{12}\right) g_{c,12j-\tau+1}. \tag{1}$$

Finally, we assume a multiplicative *iid* measurement-error model for the level of annual consumption, which implies that, after taking log differences,

$$g_{c,(j)}^{a,o} = g_{c,(j)}^a + \sigma_\epsilon^a\left(\epsilon_{(j)}^a - \epsilon_{(j-1)}^a\right). \tag{2}$$

[6] In principle we could utilize the quarterly consumption growth data from 1947 to 1959, but we do not in this version of the paper.

Measurement of Monthly Consumption Growth. Consistent with the practice of the Bureau of Economic Analysis, we assume that the levels of monthly consumption are constructed by distributing annual consumption over the 12 months of a year. This distribution is based on an observed monthly proxy series z_t that is assumed to provide a noisy measure of monthly consumption. The monthly levels of consumption are determined such that the growth rates of monthly consumption are proportional to the growth rates of the proxy series and monthly consumption adds up to annual consumption. A measurement-error model that is consistent with this assumption is the following:

$$\begin{aligned} g^o_{c,12(j-1)+1} &= g_{c,12(j-1)+1} + \sigma_\epsilon\big(\epsilon_{12(j-1)+1} - \epsilon_{12(j-2)+12}\big) \\ &\quad -\frac{1}{12}\sum_{m=1}^{12}\sigma_\epsilon\big(\epsilon_{12(j-1)+m} - \epsilon_{12(j-2)+m}\big) + \sigma^a_\epsilon\big(\epsilon^a_{(j)} - \epsilon^a_{(j-1)}\big) \\ g^o_{c,12(j-1)+m} &= g_{c,12(j-1)+m} + \sigma_\epsilon\big(\epsilon_{12(j-1)+m} - \epsilon_{12(j-1)+m-1}\big), \quad m = 2,\ldots,12. \end{aligned} \tag{3}$$

The term $\epsilon_{12(j-1)+m}$ can be interpreted as the error made by measuring the level of monthly consumption through the monthly proxy variable, that is, in log deviations $c_{12(j-1)+m} = z_{12(j-1)+m} + \epsilon_{12(j-1)+m}$. The summation of monthly measurement errors in the second line of (3) ensures that monthly consumption sums up to annual consumption. It can be verified that converting the monthly consumption growth rates into annual consumption growth rates according to (1) averages out the measurement errors and yields (2).

2.2 A Measurement Equation for Dividends

Dividend data are available at monthly frequency for our entire estimation period. There is a consensus in the finance literature that aggregate dividend series for a broad cross section of stocks exhibit a strong seasonality. This seasonality is generated by payout patterns which are not uniform over the calendar year. Much of this seasonality, in particular its deterministic component, can be removed by averaging observed dividend growth over the span of a year. To do, we utilize the same "tent" function as for consumption growth in (1):

$$g^{a,o}_{d,t+1} = \sum_{j=1}^{23}\left(\frac{12-|j-12|}{12}\right)g^o_{d,t-j+2}. \tag{4}$$

In order to relate $g^{a,o}_{d,t+1}$ to the model-implied dividend growth data, we apply the same tent-shaped transformation to $g_{d,t+1}$, that is,

$$g^{a}_{d,t+1} = \sum_{j=1}^{23}\left(\frac{12-|j-12|}{12}\right)g_{d,t-j+2}. \tag{5}$$

The measurement equation then takes the form

$$g^{a,o}_{d,t+1} = g^{a}_{d,t+1} + \sigma^{a}_{d,\epsilon}\epsilon^{a}_{d,t+1}. \tag{6}$$

To be chary, we allow for some additional measurement errors, which we assume to be *iid* across periods. Note that even for $\sigma^{a}_{d,\epsilon} = 0$ the measurement equation (6) does not imply that $g^{o}_{d,t+1} = g_{d,t+1}$ (note the absence of the tent transformation and the a superscript here). For instance, there could be a deterministic seasonal pattern in the observed monthly dividend growth data $g^{o}_{d,t+1}$ that is not part of the model-implied process $g_{d,t+1}$. The tent-shaped transformation would remove the seasonal component from observed data such that we are effectively equating the non-seasonal component of the observed data to the model-implied data.

2.3 Data

We use the per capita series of real consumption expenditure on nondurables and services from the NIPA tables available from the Bureau of Economic Analysis. Annual observations are available from 1929 to 2014, quarterly from 1947:Q1 to 2014:Q4, and monthly from 1959:M1 to 2014:M12. Growth rates of consumption are constructed by taking the first difference of the corresponding log series. In addition, we use monthly observations of dividends of the CRSP value-weighted portfolio of all stocks traded on the NYSE, AMEX, and NASDAQ. Dividend series are constructed on the per share basis as in Campbell and Shiller (1988b) and Hodrick (1992). Following Robert Shiller, we smooth out dividend series by aggregating 3 months values of the raw nominal dividend series.[7] We then compute real dividend growth as log difference of the adjusted nominal dividend series and subtract CPI inflation. Details are provided in the Online Appendix.

2.4 State-Space Representation and Bayesian Inference

Thus far, we have focused on the measurement equations that related observed cash flow growth to "true" or model implied cash flow growth. To complete the specification of the state-space model, we need to specify a law of motion for $g_{c,t}$ and $g_{d,t}$. In our empirical analysis we consider several specifications. The most comprehensive one, which is then also embedded in the asset pricing

[7] We follow Shiller's approach despite the use of the annualization in (6) because we found that the annualization did not remove all the anomalies in the data.

model, in Section 5 is the following:

$$\begin{aligned} g_{c,t+1} &= \mu_c + x_t + \sigma_{c,t}\eta_{c,t+1} \\ x_{t+1} &= \rho x_t + \sqrt{1-\rho^2}\sigma_{x,t}\eta_{x,t+1} \\ g_{d,t+1} &= \mu_d + \phi x_t + \pi\sigma_{c,t}\eta_{c,t+1} + \sigma_{d,t}\eta_{d,t+1}, \\ \sigma_{i,t} &= \varphi_i\sigma\exp(h_{i,t}), \quad h_{i,t+1} = \rho_{h_i}h_{i,t} + \sigma_{h_i}w_{i,t+1}, \quad i = \{c,x,d\}. \end{aligned} \tag{7}$$

We assume that the innovations are distributed according to

$$\eta_{i,t+1}, w_{i,t+1} \sim iid\, N(0,1)$$

and we normalize $\varphi_c = 1$.

Specification (7) is based on Bansal and Yaron (2004) and decomposes consumption growth, $g_{c,t+1}$, into a persistent component, x_t, and a transitory component, $\sigma_{c,t}\eta_{c,t+1}$. The dynamics for the persistent conditional mean follow an AR(1) with its own stochastic volatility process. Dividend streams have levered exposures to both the persistent and transitory component in consumption which is captured by the parameters ϕ and π, respectively. We allow $\sigma_{d,t}\eta_{d,t+1}$ to capture idiosyncratic movements in dividend streams. Relative to Bansal and Yaron (2004), the volatility dynamics contain three separate volatility processes. More importantly, the logarithm of the volatility process is assumed to be normal, which ensures that the standard deviation of the shocks remains positive at every point in time.

We now have a complete state-space representation. It comprises the measurement equations for consumption growth, (2) and (3), the measurement equation for dividend growth (6), and the state-transition equation (7). The state variables are model-implied monthly consumption and dividend growth and the latent volatility processes $h_{i,t}$. As econometricians who are estimating the model, we have to rely on the statistical agency to release the consumption growth data. While the statistical agency may have access to the monthly proxy series z_t in real time, it can only release the monthly consumption series that is consistent with the corresponding annual consumption observation at the end of each year. The fact that not all variables are observed in every period leads to a fairly elaborate state-space representation that is presented in the Online Appendix.

The model parameters and the latent stochastic volatilities can be summarized as follows:

$$\Theta = \big(\Theta_c, \Theta_d, \Theta_h\big), \quad H^T = \big(h_c^T, h_d^T\big), \tag{8}$$

where

$$\Theta_c = \big(\mu_c, \rho, \varphi_x, \sigma, \sigma_\epsilon, \sigma_\epsilon^a\big), \quad \Theta_d = \big(\mu_d, \phi, \varphi_d, \pi, \sigma_{d,\epsilon}^a\big), \quad \Theta_h = \big(\rho_{h_c}, \sigma_{h_c}^2, \rho_{h_d}, \sigma_{h_d}^2\big).$$

Initially, when using only consumption and dividend growth data, we restrict $h_{x,t} = h_{c,t}$ because it is not feasible to sharply identify three separate volatility processes based on cash flow data only. Throughout this paper, we will use a Bayesian approach to make inference about Θ and the latent volatilities H^T. While the law of motion of the volatilities H^T is part of the model specification (7), Bayesian inference requires a prior distribution $p(\Theta)$. According to Bayes' Theorem, the joint posterior density of parameters and latent volatilities is proportional ($\propto$)

$$p(\Theta, H^T|Y) \propto p(Y|H^T, \Theta)p(H^T|\Theta)p(\Theta). \tag{9}$$

We use MCMC methods to generate a sequence of draws $\{\Theta^{(s)}, (H^T)^{(s)}\}_{s=1}^{n_{sim}}$ from the posterior distribution.

The MCMC algorithm iterates over three conditional distributions: First, a Metropolis-Hastings step is used to draw from the posterior of $\left(\Theta_c, \Theta_d\right)$ conditional on $\left(Y, (H^T)^{(s)}, \Theta_h^{(s-1)}\right)$ Second, we draw the sequence of stochastic volatilities H^T conditional on $\left(Y, \Theta_c^{(s)}, \Theta_d^{(s)}, \Theta_h^{(s-1)}\right)$ using the algorithm developed by Kim, Shephard, and Chib (1998). It consists of transforming a nonlinear and non-Gaussian state space form into a linear and approximately Gaussian one, which allows the use of simulation smoothers such as those of Carter and Kohn (1994) to recover estimates of the residuals $\eta_{i,t}$. Finally, we draw from the posterior of the coefficients of the stochastic volatility processes, Θ_h, conditional on $\left(Y, H^{T(s)}, \Theta_c^{(s)}, \Theta_d^{(s)}\right)$.

3 Empirical Results Based on Cash Flow Data

The subsequent analysis is divided into two parts. In Section 3.1 we use only consumption data. We estimate the persistent component in consumption growth. We highlight the need for modeling measurement errors and the benefits of time aggregation in identifying this component. In Section 3.2 we show the additional information that is gained by using dividends data in conjunction with consumption in estimating the persistent component in the conditional mean and volatility dynamics of cash flows.

3.1 Estimation with Consumption Data Only

In this subsection we show the importance of accounting for measurement errors in identifying a persistent component in consumption growth. We also illustrate the informational gain through using high-frequency information and allowing for stochastic volatility. Finally, we explore a mixed-frequency approach based on a sample that contains annual consumption growth data from 1930 to 1959 and monthly data from 1960:M1 to 2014:M12.

Figure 1: Sample Autocorrelation

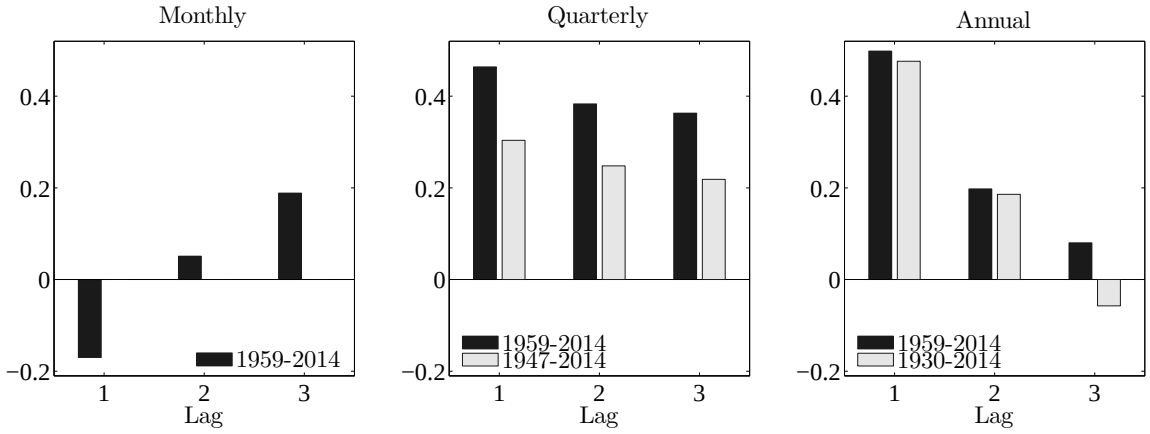

Notes: Monthly data available from 1959:M2 to 2014:M12, quarterly from 1947:Q2 to 2014:Q4, annual from 1930 to 2014.

The Role of Measurement Errors. Figure 1 displays the sample autocorrelation of consumption growth for monthly, quarterly and annual data respectively. The figure clearly demonstrates that at the annual frequency consumption growth is strongly positively autocorrelated while at the monthly frequency consumption growth has a negative first autocorrelation. These autocorrelation plots provide prima facie evidence for a negative moving average component at the monthly frequency, which is consistent with the measurement error model described in Section 2.1. Our measurement error model can reconcile the monthly negative autocorrelation with a strongly positive autocorrelation for time aggregated annual consumption. The right panel in Figure 1 also shows that the strong positive autocorrelation in annual consumption growth is robust to using the long pre-war sample as well as the post war data. Given these features of the data, we focus our analysis of measurement errors in consumption using the post 1959 monthly series.

We simplify the law of motion of cash flows in (7) by omitting dividends and assuming that the innovations are homoskedastic. Thus, the dynamics of consumption growth are reduced to the following state-space specification:

$$\begin{aligned} g^o_{c,t+1} &= \mu_c + x_t + \sigma\eta_{c,t+1} + \text{measurement error} \\ x_{t+1} &= \rho x_t + \sqrt{1-\rho^2}(\varphi_x\sigma)\eta_{x,t+1}. \end{aligned} \tag{10}$$

We will now document the effect of the measurement error specification on the estimate of ρ. Before conducting a Bayesian analysis, we examine some important features of the likelihood function. To isolate the role of measurement errors for inference about ρ, we set μ_c to the sample mean and fix σ and σ_ϵ to their respective maximum likelihood estimates, while varying the two parameters, ρ

Figure 2: Log-Likelihood Contour

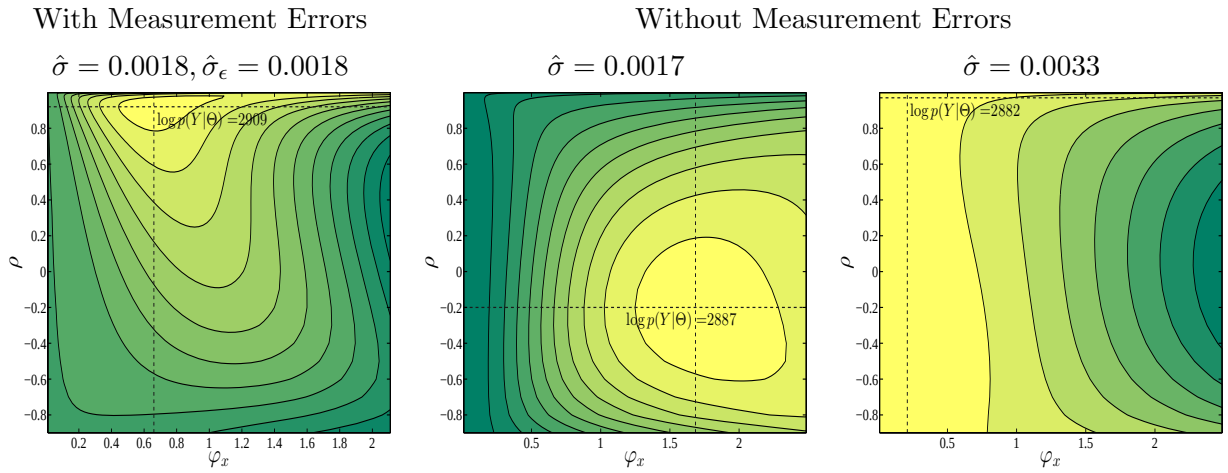

Notes: We use maximum likelihood estimation to estimate the simplified model (10) with and without allowing for measurement errors. We then fix $\sigma = \hat{\sigma}$ and $\sigma_\epsilon = \hat{\sigma}_\epsilon$ at their point estimates and vary ρ and φ_x to plot the log-likelihood function contour. Without measurement errors, we find that the log-likelihood function is bimodal at positive and negative values of ρ. Therefore, we obtain two sets of $\hat{\sigma}$.

and φ_x, that govern the dynamics of x_t.

In Figure 2 we plot likelihood function contours with and without allowing for measurement errors. In the absence of measurement errors the log-likelihood function is bimodal. The first mode is located at $\rho = -0.23$ which matches the negative monthly sample autocorrelation (see Figure 1). The location of the second mode is at $\rho = 0.96$, but the log-likelihood function is flat across a large set of values of ρ between -1 and 1. Importantly, when we allow for monthly measurement errors according to (3), setting $\sigma_\epsilon^a = 0$, the log likelihood function has a very sharp peak, displaying a very persistent expected consumption growth process with $\rho = 0.92$. Measurement errors at the monthly frequency help identify a large persistent component in consumption by allowing the model to simultaneously match the negative first-order autocorrelation observed at the monthly frequency and the large positive autocorrelation at the annual frequency.

We now proceed with the Bayesian estimation of (10) under various assumptions on the measurement error process. Table 1 reports quantiles of the prior distribution[8] as well as posterior median estimates of the model parameters. The prior for the persistence of the predictable consumption growth component is uniform over the interval $(-1, 1)$ and encompasses values that imply near

[8]In general, our priors attempt to restrict parameter values to economically plausible magnitudes. The judgment of what is *economically plausible* is, of course, informed by some empirical observations, in the same way the choice of the model specification is informed by empirical observations.

Table 1: Posterior Median Estimates of Consumption Growth Processes

	Prior Distribution				Posterior Estimates						
					State-Space Model / Measurement Error Spec.					IID	ARMA
					M&A	No ME	M	M $\rho_\epsilon > 0$	M NoAveOut		(1,2)
	Distr.	5%	50%	95%	(1)	(2)	(3)	(4)	(5)	(6)	(7)
μ	N	-.007	.0016	.0100	.0016	.0016	.0016	.0016	.0016	.0016	.0016
ρ	U	-.90	0	.90	.917	-.229	.917	.916	.914	-	.915
φ_x	U	.1	1.0	1.9	.740	1.67	.707	.714	.753	-	-
σ	IG	.0008	.0019	.0061	.0017	.0017	.0018	.0018	.0017	.0033	.0032
σ_ϵ	IG	.0008	.0019	.0061	.0018	-	.0018	.0018	.0019	-	-
σ_ϵ^a	IG	.0007	.0029	.0386	.0014	-	-	-	-	-	-
ρ_ϵ	U	-.90	0	.90	-	-	-	.013	-	-	-
ζ_1	N	-8.2	0	8.2	-	-	-	-	-	-	-1.14
ζ_2	N	-8.2	0	8.2	-	-	-	-	-	-	.301
$\ln p(Y)$					2898.4	2878.2	2897.8	2894.5	2898.5	2871.0	2891.3

Notes: The estimation sample is from 1959:M2 to 2014:M12. We denote the persistence of the growth component by ρ and the persistence of the measurement errors by ρ_ϵ. We report posterior median estimates for the following measurement error specifications of the state-space model: (1) monthly and annual measurement errors (M&A); (2) no measurement errors (no ME); (3) monthly measurement errors (M); (4) serially correlated monthly measurement errors (M, $\rho_\epsilon > 0$); (5) monthly measurement errors that do not average out at annual frequency (M, NoAveOut). In addition we report results for the following models: (6) consumption growth is *iid*; (7) consumption growth is ARMA(1,2).

iid consumption growth as well as values for which x_t is almost a unit root process. The consumption growth process (10) implies that the parameter φ_x can be interpreted as the square root of a "signal-to-noise ratio," meaning the ratio of the variance of x_t over the variance of the *iid* component $\sigma\eta_{c,t+1}$. We use a uniform prior for φ_x that allows for "signal-to-noise ratios" between 0 and 1. At an annualized rate, our *a priori* 90% credible interval for σ and σ_ϵ ranges from 0.3% to 2.1% and the prior for the σ_ϵ^a covers the interval 0.07% to 3.9%. For comparison, the sample standard deviations of annualized monthly consumption growth and annual consumption growth are approximately 1.1% and 2%.

Our posterior estimates confirm the graphical pattern in Figure 2. With monthly measurement errors the posterior median of ρ is approximately 0.92. In the absence of measurement errors, it drops to -0.23. We conclude from Table 1 that allowing for measurement errors reveals a very persistent component in consumption growth. This conclusion is by no means an artifact of tight

priors since priors for both persistence and the standard deviation ratio are flat. At first glance, the large estimate of ρ may appear inconsistent with the negative sample autocorrelation of monthly consumption growth reported in Figure 1. However, the sample moment confounds the persistence of the "true" consumption growth process and the dynamics of the measurement errors. Our state-space framework is able to disentangle the various components of the observed monthly consumption growth, thereby detecting a highly persistent predictable component x_t that is hidden under a layer of measurement errors.

Our inference about ρ is robust to the choice of measurement error model. We consider (1) our benchmark specification of monthly and annual measurement errors; (3) only monthly measurement errors; (4) serially correlated monthly measurement errors; and (5) monthly measurement errors that do not cancel out at annual frequency. The posterior median estimates of ρ are essentially the same for these four specifications. To provide formal support for our choice of benchmark specification, we also report log marginal data densities in the bottom row of the table. Accounting for numerical approximation errors specification (1) is essentially at par with specification (5) and these two specifications dominate all alternatives. We find specification (1) conceptually more appealing than (5). In the last two columns of Table 1 we report results for a model that assumes that consumption growth is *iid* and for an ARMA(1,2) model. The latter nests the no-measurement error specification (2) and specification (5) in which monthly measurement errors do not average out at the annual frequency. A log marginal data density differential of 27.4 between specifications (1) and (6) indicates that monthly consumption growth is clearly not *iid*. Moreover, our benchmark measurement error specification also dominates the ARMA(1,2) model in terms of fit, again highlighting the importance of measurement errors. The log marginal data density differential is 7.1.

In order to examine the degree to which measurement errors contribute to the variation in the observed consumption growth, we conduct variance decomposition of monthly and annual consumption growth using measurement error specification of column (1) in Table 1. We find that more than half of the observed monthly consumption growth variation is due to measurement errors. For annual consumption growth data, this fraction drops below 1%. On the other hand, the opposite pattern holds true for the persistent growth component. While the variation in the persistent growth component only accounts for 13% of the monthly consumption growth variation, this fraction increases to 87% for annual consumption growth data.

Informational Gain Through Temporal Disaggregation and Stochastic Volatility. The observation that monthly consumption growth data are strongly contaminated by measurement errors which to a large extent average out at quarterly or annual frequency, suggests that one

Table 2: Informational Gain Through High-Frequency Observations

Data Frequency	Posterior of ρ 5%	50%	95%	90% Intv. Width
Without Stochastic Volatility				
Monthly	.847	.917	.963	.116
Quarterly	.783	.891	.958	.175
Annual	.539	.803	.928	.389
With Stochastic Volatility				
Monthly	.904	.951	.980	.076
Quarterly	.856	.921	.963	.107

Notes: The estimation sample ranges from 1959:M2 to 2014:M12. The model frequency is monthly. For monthly data we use both monthly and annual measurement errors (specification (1) in Table 1). For quarterly (annual) data we use quarterly (annual) measurement errors only. The specifications of the models without and with stochastic volatility are given in (10) and (11), respectively.

might be able to estimate ρ equally well based on time-aggregated data. We examine this issue in Table 2. The first row reproduces the ρ estimate from Specification (1) of Table 1. However, we now also report the 5% and 95% quantile of the posterior distribution. Keeping the length of a period equal to a month in the state-space model, we change the measurement equation to link it with quarterly and annual consumption growth data. As the data frequency drops from monthly to annual, the posterior median estimate of ρ falls from 0.92 to 0.80. Moreover, the width of the equal-tail probability 90% credible interval increases from 0.11 to 0.39, highlighting that the use of high-frequency data sharpens inference about ρ.

The original cash flow model in (7) assumes that the innovations are heteroskedastic. Thus, we now re-estimate the state-space model for consumption growth, allowing for a common stochastic volatility process for $\eta_{c,t}$ and $\eta_{x,t}$ in (10):

$$\begin{aligned} g^o_{c,t+1} &= \mu_c + x_t + \sigma_{c,t}\eta_{c,t+1} + \text{measurement error} \\ x_{t+1} &= \rho x_t + \sqrt{1-\rho^2}\varphi_x \sigma_{c,t}\eta_{x,t+1} \\ \sigma_{c,t} &= \sigma \exp(h_{c,t}), \quad h_{c,t+1} = \rho_{h_c} h_{c,t} + \sigma_{h_c} w_{c,t+1}. \end{aligned} \tag{11}$$

In view of (7) we are imposing $h_{x,t} = h_{c,t}$, which facilitates the identification of the volatility process and its parameters. Our prior interval for the persistence of the volatility processes ranges from

0.27 to 0.999. The prior for the standard deviation of the consumption volatility process implies that the volatility may fluctuate either relatively little, over the range of 0.7 to 1.2 times the average volatility, or substantially, over the range of 0.4 to 2.4 times the average volatility.

The width of the 90% credible interval for ρ shrinks from 0.116 to 0.076 for monthly data and from 0.175 to 0.107 for quarterly data.[9] At the same time the posterior median of ρ increases from 0.917 to 0.951 for monthly data and from 0.891 to 0.921 for quarterly data. Without stochastic volatility sharp movements in consumption growth must be accounted for by large temporary shocks reducing the estimate of ρ; however, the presence of stochastic volatility allows the model to account for these sharp movements by fluctuations in the conditional variance of the shocks enabling ρ to be large. We conclude that allowing for heteroskedasticity reduces the posterior uncertainty about ρ and raises the point estimate.

As a by-product, we also obtain an estimate for the persistence, ρ_{h_c}, of the stochastic volatility process in (11). The degree of serial correlation of the volatility also has important implications for asset pricing. Starting from a truncated normal distribution that implies a 90% prior credible set ranging from 0.27 to 0.99, based on monthly observations the posterior credible set ranges from 0.955 to 0.999, indicating that the data favor a highly persistent volatility process $h_{c,t}$. Once the observation frequency is reduced from monthly to quarterly the sample contains less information about the high frequency volatility process and there is less updating of the prior distribution. Now the 90% credible interval ranges from 0.41 to 0.97.

Hansen, Heaton, and Li (2008) estimate a cointegration model for log consumption and log earnings to extract a persistent component in consumption. The length of a time period in their reduced-rank vector autoregression (VAR) is a quarter and the model is estimated based on quarterly data. The authors find that the ratio of long-run to short-run response of log consumption to a persistent growth shock, $\eta_{x,t}$ in our notation, is about two, which would translate into an estimate of ρ of approximately 0.5 for a quarterly model. As a robustness check, we estimate three quarterly versions of the state-space model (11): without quarterly measurement errors and with homoskedastic innovations, with quarterly measurement errors and homoskedastic innovations, and with quarterly measurement errors and stochastic volatility. The posterior median estimates of ρ are 0.649, 0.676, and 0.735, respectively. These results are by and large consistent with the low value reported in Hansen, Heaton, and Li (2008) as well as the estimate in Hansen (2007) under the "loose" prior. Using a crude cube-root transformations, the quarterly ρ estimates translate into 0.866, 0.878, and 0.903 at monthly frequency and thereby somewhat lower than the estimates

[9] We found that the state-space model with stochastic volatility is poorly identified if the observation frequency is annual, which is why we do not report this case in Table 1.

obtained by estimating a monthly model on quarterly data.

Estimation Based on Mixed-Frequency Data. Thus far, we have utilized data starting in 1960. However, to measure the small persistent component in consumption growth, one would arguably want to use the longest span of data possible. Thus, we now extend the sample to include data going back to 1930. Unfortunately, prior to 1959:M2 monthly consumption growth data are unavailable. Thus, we adopt a mixed-frequency approach that utilizes annual data from 1930 to 1959 and then switches to monthly data afterwards.

It is well known from Romer (1986) and Romer (1989) that prewar data on consumption are known to be measured with significantly greater error that exaggerates the size of cyclical fluctuations. To cope with the criticism, we allow for annual measurement errors during 1930-1948 but restrict them to be zero afterwards. This break in measurement errors is also motivated by Amir-Ahmadi, Matthes, and Wang (2016) who provide empirical evidence for larger measurement in the early sample before the end of World War II. Importantly, we always account for monthly measurement errors whenever we use monthly data.

Prior credible intervals and posterior estimates are presented in Table 3. Note that the ρ estimate reported under the 1959:M2-2014:M12 posterior is the same as the estimate reported in Table 2 based on monthly data and the model with stochastic volatility. Extending the sample period reduces the posterior median estimate of ρ slightly, from 0.95 to 0.94. We attribute this change to the large fluctuations around the time of the Great Depression. The width of the credible interval stays approximately the same. Note that at this stage we are adding 30 annual observations to a sample of 671 monthly observations (and we are losing 11 monthly observations from 1959). The standard deviation of the monthly measurement error σ_ϵ is estimated to be about half of σ and is robust to different estimation samples because it is solely identified from monthly consumption growth data. The standard deviation of the annual measurement error is larger than that of monthly measurement error by a factor of 4 (recall that to compare σ_ϵ and σ_ϵ^a one needs to scale the latter by $\sqrt{12}$). This finding is consistent with Amir-Ahmadi, Matthes, and Wang (2016) who find significant presence of measurement errors in output growth during 1930 and 1948.

3.2 Estimation with Consumption and Dividend Data

We now include dividend growth data in the estimation of the cash flow model. We proceed with the mixed-frequency approach and combine the monthly dividend growth data with annual consumption growth data from 1930 to 1959 and monthly data from 1960:M1 to 2014:M12. Table 4 provides percentiles of the prior distribution and the posterior distribution for the post 1959 estimation sample and for the mixed frequency sample starting in 1930. The priors for ϕ and π,

Table 3: Posterior Estimates: Consumption Only

		Prior			Posterior			Posterior		
								1930-1959		
					1959:M2-2014:M12			1960:M1-2014:M12		
	Distr.	5%	50%	95%	5%	50%	95%	5%	50%	95%
Consumption Growth Process										
μ_c	N	-.007	.0016	.0100	.0009	.0016	.0019	.0010	.0016	.0018
ρ	U	-.9	0	.9	.904	.951	.980	.891	.940	.971
φ_x	U	.05	.50	.95	.357	.509	.778	.369	.535	.759
σ	IG	.0008	.0019	.0061	.0017	.0021	.0025	.0017	.0022	.0028
ρ_{h_c}	N^T	.27	.80	.999	.955	.988	.999	.949	.984	.996
$\sigma^2_{h_c}$	IG	.0011	.0060	.0283	.0007	.0014	.0030	.0022	.0054	.0242
Consumption Measurement Error										
σ_ϵ	IG	.0008	.0019	.0061	.0010	.0013	.0016	.0010	.0013	.0016
σ^a_ϵ	IG	.0007	.0029	.0386	.0010	.0015	.0020	.0010	.0198	.0372

Notes: We report estimates of model (11). We adopt the measurement error model of Section 2.1. N, N^T, G, IG, and U denote normal, truncated (outside of the interval $(-1, 1)$) normal, gamma, inverse gamma, and uniform distributions, respectively. We allow for annual consumption measurement errors ϵ^a_t during the periods from 1930 to 1948. We impose monthly measurement errors ϵ_t when we switch from annual to monthly consumption data from 1960:M1 to 2014:M12.

parameters that determine the comovement of dividend and consumption growth, are uniform distributions on the interval [0, 10]. The parameter φ_d determines the standard deviation of the *iid* component of dividend growth relative to consumption growth. Here we use a prior that is uniform on the interval [0, 10], thereby allowing for dividends to be much more volatile than consumption. The prior for the standard deviation of the dividend volatility process implies that the volatility may fluctuate either relatively little, over the range of 0.5 to 2.1 times the average volatility, or substantially, over the range of 0.1 to 13 times the average volatility. Finally, we fix the measurement error standard deviation $\sigma_{d,\epsilon}$ at 10% of the sample standard deviation of dividend growth.

The most important finding is that the posterior median ρ increases as we add dividend growth data in the estimation. In addition, we find significant reduction in our uncertainty about ρ captured by the distance between 95% and 5% posterior quantiles. The posterior median of ρ is around 0.97 for the post 1959 sample and is 0.95 for the longer sample, both of which are higher than those

Table 4: Posterior Estimates: Consumption and Dividend Growth

		Prior			Posterior			Posterior		
								1930-1959		
					1959:M2-2014:M12			1960:M1-2014:M12		
	Distr.	5%	50%	95%	5%	50%	95%	5%	50%	95%
Consumption Growth Process										
ρ	U	-.90	0	.90	.935	.968	.991	.913	.950	.978
φ_x	U	.05	.50	.95	.282	.439	.636	.267	.435	.624
σ	IG	.0008	.0019	.0061	.0019	.0022	.0025	.0022	.0026	.0034
ρ_{h_c}	N^T	.27	.80	.999	.948	.983	.997	.974	.991	.998
$\sigma^2_{h_c}$	IG	.0011	.0060	.0283	.0017	.0062	.0225	.0010	.0042	.0104
Dividend Growth Process										
ϕ	U	.50	5.0	9.50	1.66	2.77	4.26	1.81	2.94	4.80
π	U	.50	5.0	9.50	.033	.317	.991	.027	.286	.849
φ_d	U	.50	5.0	9.50	3.14	4.62	6.21	2.85	4.98	6.91
ρ_{h_d}	N^T	.27	.80	.999	.943	.976	.993	.943	.973	.989
$\sigma^2_{h_d}$	IG	.015	.0445	.208	.0188	.0453	.1061	.0229	.0476	.1229
Consumption Measurement Error										
σ_ϵ	IG	.0008	.0019	.0062	.0010	.0012	.0015	.0009	.0012	.0014
σ^a_ϵ	IG	.0042	.0120	.0564	-	-	-	.0065	.0129	.0218

Notes: We utilize the mixed-frequency approach in the estimation: For consumption we use annual data from 1930 to 1959 and monthly data from 1960:M1 to 2014:M12; we use monthly dividend annual growth data from 1930:M1 to 2014:M12. For consumption we adopt the measurement error model of Section 2.1. We allow for annual consumption measurement errors ϵ^a_t during the periods from 1930 to 1948. We impose monthly measurement errors ϵ_t when we switch from annual to monthly consumption data from 1960:M1 to 2014:M12. We fix $\mu_c = 0.0016$ and $\mu_d = 0.0010$ at their sample averages. Moreover, we fix the measurement error standard deviation $\sigma^a_{d,\epsilon}$ at 10% of the sample standard deviation of dividend growth. N, N^T, G, IG, and U denote normal, truncated (outside of the interval $(-1, 1)$) normal, gamma, inverse gamma, and uniform distributions, respectively.

in Table 3. The 5-95% distance dropped from 0.075 to 0.055 as we include dividend growth in the estimation (compare with Table 3). The posterior median of the standard deviation of the unconditional volatility of the persistent component φ_x is around 0.44, slightly lower than before.

The dividend leverage ratio on expected consumption growth ϕ is estimated to be around 2.8 and the standard deviation of the idiosyncratic dividend shocks φ_d is around 5. The estimation

results also provide strong evidence for stochastic volatility. According to the posteriors reported in Table 4, both $\sigma_{c,t}$ and $\sigma_{d,t}$ exhibit significant time variation. The posterior medians of ρ_{h_c} and ρ_{h_d} range from 0.97 to 0.99. Overall, the magnitude of parameter estimates are quite close to the values used in the LRR literature (see Bansal, Kiku, and Yaron (2012)).

4 The Long-Run Risks Model

We now embed the cash flow process (7) into an endowment economy, which allows us to price financial assets. The preferences of the representative household are described in Section 4.1. Section 4.2 describes the model solution. Section 4.3 presents the state-space representation of the asset-pricing model and its Bayesian estimation.

4.1 Representative Agent's Optimization

We consider an endowment economy with a representative agent that has Epstein and Zin (1989) recursive preferences and maximizes her lifetime utility,

$$V_t = \max_{C_t} \left[(1-\delta)\lambda_t C_t^{\frac{1-\gamma}{\theta}} + \delta\big(\mathbb{E}_t[V_{t+1}^{1-\gamma}]\big)^{\frac{1}{\theta}} \right]^{\frac{\theta}{1-\gamma}},$$

subject to budget constraint

$$W_{t+1} = (W_t - C_t)R_{c,t+1},$$

where W_t is the wealth of the agent, $R_{c,t+1}$ is the return on all invested wealth, γ is risk aversion, $\theta = \frac{1-\gamma}{1-1/\psi}$, and ψ is intertemporal elasticity of substitution. As highlighted in Albuquerque, Eichenbaum, Luo, and Rebelo (2016), we also allow for a preference shock, λ_t, to the time rate of preference. The endowment stream is given by the law of motion for consumption and dividend growth in (7), and the growth rate of the preference shock, denoted by $x_{\lambda,t}$, follows an AR(1) process with shocks that are independent of the shocks to cash flows:

$$x_{\lambda,t+1} = \rho_\lambda x_{\lambda,t} + \sigma_\lambda \eta_{\lambda,t+1}, \quad \eta_{\lambda,t+1} \sim iidN(0,1). \tag{12}$$

The Euler equation for any asset $r_{i,t+1}$ takes the form

$$\mathbb{E}_t\left[\exp\left(m_{t+1} + r_{i,t+1}\right)\right] = 1, \tag{13}$$

where $m_{t+1} = \theta \log\delta - \frac{\theta}{\psi} g_{c,t+1} + (\theta - 1) r_{c,t+1}$ is the log of the real stochastic discount factor (SDF), and $r_{c,t+1}$ is the log return on the consumption claim. We reserve $r_{m,t+1}$ for the log market return – the return on a claim to the market dividend cash flows.[10]

[10]Formally, markets are complete in the sense that all income and assets are tradable and add up to total wealth for which the return is $R_{c,t}$. In particular, let $R_{j,t+1} = (d_{j,t+1} + p_{j,t+1})/p_{j,t}$ be the return to a claim that pays the

4.2 Solution

Given the cash flow dynamics in (7) and the Euler equation (13), we derive asset prices using the approximate analytical solution described in Bansal, Kiku, and Yaron (2012) which utilizes the Campbell and Shiller (1988a) log-linear approximation for returns. However, because the volatility processes in (7) do not follow normal distributions, an analytical expression to (13) is infeasible.[11] To accommodate an analytical solution, we utilize a linear approximation to (7) and express volatility in (14) as a process that follows Gaussian dynamics:

$$\begin{aligned} \sigma_{i,t}^2 - (\varphi_i\sigma)^2 &= 2(\varphi_i\sigma)^2 h_{i,t} + O(|h_{i,t}^2|), \quad h_{i,t+1} = \rho_{h_i} h_{i,t} + \sigma_{h_i} w_{i,t+1} \\ \sigma_{i,t+1}^2 &\approx (\varphi_i\sigma)^2(1-\rho_{h_i}) + \rho_{h_i}\sigma_{i,t}^2 + (2(\varphi_i\sigma)^2\sigma_{h_i}) w_{i,t+1} \\ &= (\varphi_i\sigma)^2(1-\nu_i) + \nu_i\sigma_{i,t}^2 + \sigma_{w_i} w_{i,t+1}, \quad i = \{c, x, d\}. \end{aligned} \tag{14}$$

The analytical solution afforded via this pseudo-volatility process is important since it facilitates estimation (see details below).

The solution to the log price-consumption ratio follows, $pc_t = A_0 + A_1 x_t + A_{1,\lambda} x_{\lambda,t} + A_{2,c}\sigma_{c,t}^2 + A_{2,x}\sigma_{x,t}^2$. As discussed in Bansal and Yaron (2004), $A_1 = \frac{1-\frac{1}{\psi}}{1-\kappa_1\rho}$, the elasticity of prices with respect to growth prospects, will be positive whenever the IES, ψ, is greater than 1. $A_{1,\lambda} = \frac{\rho_\lambda}{1-\kappa_1\rho_\lambda}$, the elasticity of prices with respect to the growth rate of the preference shock, is always positive. Further, the elasticity of pc_t with respect to the two volatility processes $\sigma_{c,t}^2$ and $\sigma_{x,t}^2$ is $\frac{\theta}{2}\frac{(1-\frac{1}{\psi})^2}{1-\kappa_1\nu_c}$ and $\frac{\theta}{2}\frac{(\kappa_1 A_1)^2}{1-\kappa_1\nu_x}$ respectively; both will be negative — namely, prices will decline with uncertainty — whenever θ is negative. A condition that guarantees a negative θ is that agents have a preference for early resolution of uncertainty. The innovation to the log stochastic discount factor (SDF) are linear in the shocks to consumption growth (η_c, η_x, η_λ, w_c, w_x), with λs denoting their respective market prices of risk (the derivation given in Appendix C). It is instructive to note that $\lambda_c = -\gamma$, $\lambda_x = \frac{-(\gamma-\frac{1}{\psi})\kappa_1}{1-\kappa_1\rho}$, $\lambda_\lambda = \frac{\theta-\kappa_1\rho_\lambda}{1-\kappa_1\rho_\lambda}$ (and λ_{w_c} and λ_{w_x}) are negative (positive) whenever preferences exhibit early resolution of uncertainty $\gamma > 1/\psi$. Furthermore the λs (except λ_c) will be zero when preferences are time separable, namely, when $\theta = 1$.

dividend stream $\{d_{j,\tau}\}_{\tau=t}^{\infty}$ and has the price $p_{j,t}$. Let $q_{j,t}$ be the number of shares. Then $W_t - C_t = \sum_j p_{j,t}q_{j,t}$. Wealth next period, W_{t+1}, equals $\sum_j p_{j,t}q_{j,t}R_{j,t+1}$, and it follows that $R_{c,t+1} = \frac{\sum_j p_{j,t}q_{j,t}R_{j,t+1}}{\sum_j p_{j,t}q_{j,t}}$. As in Lucas (1978), we normalize all shares $q_{j,t}$ to one and the risk free asset to be in zero net supply such that in equilibrium $C_t = D_m + D_o$, where D_m are the dividends to all tradable financial assets and D_o are dividends on all other assets (e.g., labor, housing etc.). R_m, the return we utilize in our empirical work, is the return on the claims that pay dividends D_m.

[11] Strictly speaking, to guarantee the existence of conditional moments involved in key equilibrium conditions, the exponential function $\sigma_{i,t} = \varphi_i\sigma\exp(h_{i,t})$ in (7) needs to be spliced together with a non-exponential function, e.g., a square-root function, for volatilities $h_{i,t}$ exceeding some large threshold $\bar{h}_i$. See Chernov, Gallant, Ghysels, and Tauchen (2003) and Andreasen (2010).

Risk premia are determined by the negative covariation between the innovations to returns and the innovations to the SDF. It can be shown that the risk premium for the market return, $r_{m,t+1}$, is

$$\begin{aligned}\mathbb{E}_t(r_{m,t+1} - r_{f,t}) + \frac{1}{2}var_t(r_{m,t+1}) &= -cov_t(m_{t+1}, r_{m,t+1}) \\ &= \underbrace{\beta_{m,c}\lambda_c\sigma^2_{c,t}}_{\text{short-run risk}} + \underbrace{\beta_{m,x}\lambda_x\sigma^2_{x,t}}_{\text{long-run growth risk}} + \underbrace{\beta_{m,\lambda}\lambda_\lambda\sigma^2_{\lambda}}_{\text{preference risk}} \\ &\quad + \underbrace{\beta_{m,w_x}\lambda_{w_x}\sigma^2_{w_x} + \beta_{m,w_c}\lambda_{w_c}\sigma^2_{w_c}}_{\text{volatility risks}},\end{aligned} \tag{15}$$

where the βs are given in Appendix C and reflect the exposures of the market return to the underlying consumption risks. Equation (15) highlights that the conditional equity premium can be attributed to (i) short-run consumption growth, (ii) long-run growth, (iii) preference shocks, (iv) short-run and long-run volatility risks.

A key variable for identifying the model parameters is the risk-free rate. Under the assumed dynamics in (7), the risk-free rate is affine in the state variables and follows

$$r_{f,t} = B_0 + B_1 x_t + B_{1,\lambda} x_{\lambda,t} + B_{2,c}\sigma^2_{c,t} + B_{2,x}\sigma^2_{x,t},$$

where the Bs are derived in the Online Appendix. It is worth noting that $B_1 = \frac{1}{\psi} > 0$ and the risk-free rate rises with good economic prospects, while $B_{1,\lambda} = -\rho_\lambda < 0$ and the risk-free rate falls with positive preference shock. Under $\psi > 1$, $\gamma > 1$ and whenever preferences exhibit early resolution of uncertainty, $B_{2,c}$ and $B_{2,x}$ are negative so the risk-free rate declines with a rise in economic uncertainty.

4.3 State-Space Representation and Bayesian Inference

The vector of model parameters now also encompasses the parameters that characterize the preferences of the representative household. Morever, we are utilizing the third stochastic volatility process, $h_{x,t}$. Thus, we define

$$\Theta = \big(\Theta_c, \Theta_d, \Theta_h, \Theta_m\big), \tag{16}$$

where

$$\begin{aligned}\Theta_c &= \big(\mu_c, \rho, \varphi_x, \sigma, \sigma_\epsilon, \sigma^a_\epsilon\big), \quad \Theta_d = \big(\mu_d, \phi, \varphi_d, \pi, \sigma^a_{d,\epsilon}\big), \\ \Theta_h &= \big(\rho_{h_c}, \sigma^2_{h_c}, \rho_{h_d}, \sigma^2_{h_d}, \rho_{h_x}, \sigma^2_{h_x}\big), \quad \Theta_m = \big(\delta, \psi, \gamma, \rho_\lambda, \sigma_\lambda, \sigma^{r_f}_\epsilon\big).\end{aligned}$$

Here Θ_c and Θ_d are the same as in (8), Θ_h is augmented by ρ_{h_x} and $\sigma^2_{h_x}$, and Θ_m collects the preference parameters, including those of the law of motion of the shock process λ_t in the generalized model, and the measurement error for the real rate.

Compared to the cash flow model, the state-space representation of the LRR model is significantly more elaborate. In addition to consumption and dividend growth, the vector of observables y_t now also contains the observed market return $r^o_{m,t}$ and the risk-free rate $r^o_{f,t}$. At a general level, the measurement equation takes the form

$$y_{t+1} = A_{t+1}\big(D + Zs_{t+1} + Z^v s^v_{t+1}(h_{t+1}, h_t) + \Sigma^u u_{t+1}\big), \quad u_{t+1} \sim iidN(0, I). \tag{17}$$

The vector s_{t+1} essentially consists of the persistent cash flow component x_t (see (7)) as well as $x_{\lambda,t}$. However, in order to express the observables y_{t+1} as a linear function of s_{t+1} and to account for potentially missing observations, it is necessary to augment s_{t+1} by lags of x_t and $x_{\lambda,t}$ as well as the innovations for the cash flow process. Because the details are cumbersome and at this stage non essential, a precise definition of s_{t+1} is relegated to the Online Appendix.

The vector $s^v_{t+1}(\cdot)$ is a function of the log volatilities of cash flows, h_{t+1} and h_t, in (7). Finally, u_{t+1} is a vector of measurement errors and A_{t+1} is a selection matrix that accounts for deterministic changes in the data availability. The solution of the LRR model sketched in Section 4.2 provides the link between the state variables and the observables y_{t+1}. The state variables themselves follow vector autoregressive processes of the form

$$s_{t+1} = \Phi s_t + v_{t+1}(h_t), \quad h_{t+1} = \Psi h_t + \Sigma_h w_{t+1}, \quad w_{t+1} \sim iidN(0, I), \tag{18}$$

where $v_{t+1}(\cdot)$ is an innovation process with a variance that is a function of the log volatility process h_t and w_{t+1} is the innovation of the stochastic volatility process. Equations (17) and (18) define a nonlinear state-space system in which the size of the vector of observables y_t changes in a deterministic manner.

Because in (17) the volatility states s^v_t affect the conditional mean of the observables y_t, the Metropolis-within-Gibbs sampler described in Section 2.4 cannot be used for posterior inference in the LRR model. Instead, we construct a Metropolis-Hastings sampler that generates draws from $p(\Theta|Y)$. The challenging aspect of this sampler is the evaluation of the likelihood function $p(Y|\Theta)$ associated with the nonlinear state-space model given by (17) and (18). We exploit the fact that our state-space model is linear and Gaussian conditional on the volatility states (h_{t+1}, h_t) to construct a computationally efficient particle filter approximation $\hat{p}(Y|\Theta)$ of the likelihood function (see Online Appendix for details).[12] The key feature of the algorithm is that particle values for the high-dimensional vector s_t are replaced by the mean and covariance matrix of the conditional distribution of $s_t|(h_t, h_{t-1}, Y_{1:t})$ which is Gaussian. The general idea has been previously used,

[12] Andrieu, Doucet, and Holenstein (2010) have shown that the use of $\hat{p}(Y|\Theta)$ in MCMC algorithms can still deliver draws from the actual posterior $p(\Theta|Y)$ because these approximation errors essentially average out as the Markov chain progresses.

for instance, in Chen and Liu (2000) and Shephard (2015). It reduces the variance of $\hat{p}(Y|\Theta)$ considerably, making it possible to embed the likelihood approximation into a fairly standard random-walk Metropolis algorithm that is widely used in the DSGE model literature; see Herbst and Schorfheide (2015).

5 Empirical Results Based on the Long-Run Risks Model

Section 5.1 describes the data set used in the empirical analysis. Section 5.2 describes our estimation results and Section 5.3 describes the asset pricing implications.

5.1 Data

In addition to the consumption and dividend data used in Section 3 we now also use financial market data from 1930:M1 to 2014:M12. This includes monthly observations of returns and prices of the CRSP value-weighted portfolio of all stocks traded on the NYSE, AMEX, and NASDAQ. Prices are also constructed on the per share basis as in Campbell and Shiller (1988b) and Hodrick (1992). The stock market data are converted to real using the consumer price index (CPI) from the Bureau of Labor Statistics. Finally, the ex-ante real risk-free rate is constructed as a fitted value from a projection of the ex-post real rate on the current nominal yield and inflation over the previous year. To run the predictive regression, we use monthly observations on the three-month nominal yield from the CRSP Fama Risk Free Rate tapes and CPI series. Data sources and summary statistics are available in the Online Appendix.

5.2 Model Estimation

Parameter Estimates. The prior distribution for the parameters associated with the exogenous cash flow process are the same as the ones used in Section 3.2. Thus, we focus on the preference parameters that affect the asset pricing implications of the model. Percentiles for the prior are reported in the left-side columns of Table 5. The prior for the discount rate δ reflects beliefs about the magnitude of the risk-free rate. For the asset pricing implications of our model, it is important whether the IES is below or above 1. Thus, we choose a prior that covers the range from 0.3 to 3.5. The 90% prior credible interval for the risk-aversion parameter γ ranges from 3 to 15, encompassing the values that are regarded as reasonable in the asset pricing literature. We use the same prior for the parameters of the cash flow processes and their measurement errors as in Section 3. The prior for the persistence and the innovation standard deviation of the preference shock is identical

Table 5: Prior and Posterior Estimates

		Prior			Posterior		
	Distr.	5%	50%	95%	5%	50%	95%
Household Preferences							
δ	B	.995	.9975	.9999	-	.999	-
ψ	G	.30	1.30	3.45	1.13	1.93	3.42
γ	G	2.75	7.34	15.46	5.44	8.60	12.97
Preference Risk							
ρ_λ	U	-.90	0	.90	.916	.956	.982
σ_λ	IG	.0001	.0003	.0007	.0003	.0005	.0007
Consumption Growth Process							
ρ	U	-.90	0	.90	.949	.987	.999
φ_x	U	.05	.50	.95	.139	.232	.506
σ	IG	.0008	.0019	.0061	.0020	.0032	.0044
ρ_{h_c}	N^T	.27	.80	.999	.973	.991	.996
$\sigma^2_{h_c}$	IG	.0011	.0060	.0283	.0074	.0088	.0100
ρ_{h_x}	N^T	.27	.80	.999	.987	.994	.999
$\sigma^2_{h_x}$	IG	.0011	.0060	.0283	.0027	.0039	.0061
Dividend Growth Process							
ϕ	N	.50	5.0	9.5	2.82	4.15	5.44
π	N	.50	5.0	9.5	.204	1.54	4.31
φ_d	U	.50	5.0	9.5	3.56	5.02	7.83
ρ_{h_d}	N^T	.28	.80	.999	.948	.967	.984
$\sigma^2_{h_d}$	IG	.015	.0445	.208	.0174	.0393	.0833
Consumption Measurement Error							
σ_ϵ	IG	.0008	.0019	.0062	.0006	.0010	.0016
σ^a_ϵ	IG	.0042	.0120	.0564	.0061	.0231	.0423

Notes: The estimation results are based on annual consumption growth data from 1930 to 1960 and monthly consumption growth data from 1960:M1 to 2014:M12. We allow for annual consumption measurement errors ϵ^a_t during the periods from 1930 to 1948. We impose monthly measurement errors ϵ_t when we switch from annual to monthly consumption data from 1960:M1 to 2014:M12. For the other three series we use monthly data from 1930:M1 to 2014:M12. We fix $\mu_c = 0.0016$ and $\mu_d = 0.0010$ at their sample averages. Moreover, we fix the measurement error standard deviations $\sigma^a_{d,\epsilon}$ and $\sigma_{f,\epsilon}$ at 10% of the sample standard deviation of dividend growth and the risk-free rate, respectively. B, N, N^T, G, and IG are beta, normal, truncated (outside of the interval $(-1, 1)$) normal, gamma, and inverse gamma distributions, respectively.

Figure 3: Posterior Distribution of ρ

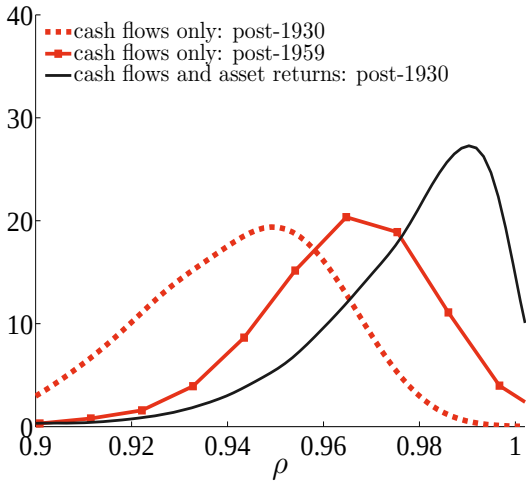

Notes: We plot posterior densities of ρ from the estimation with cash flow data only from post-1930 (red-dashed) and from post-1959 samples (red-dotted), respectively, and from the estimation with cash flow and asset return data from post-1930 sample (black).

to the prior for the cash flow parameters ρ and σ. Finally, we fix the standard deviation $\sigma_{f,\epsilon}$ of the measurement error of the risk free rate at 10% of the risk-free rate's sample standard deviation.

The remaining columns of Table 5 summarize the percentiles of the posterior distribution for the model parameters. While the estimated cash flow parameters are, by and large, similar to those reported in Table 4 when asset prices are not utilized, a few noteworthy differences emerge. First, the estimate of ρ, the persistence of the predictable cash flow component, increases from 0.950 to 0.987 to better capture the equity premium and persistence of the price-dividend ratio. Figure 3 overlays the posterior densities of ρ obtained with (post-1930 sample) and without asset prices (post-1930 and post-1959 samples, respectively).[13] Interestingly, the figure shows that although the mode of the posterior increases and shifts to the right when asset prices are used in estimation, the 90% credible interval ranging from 0.949 to 0.999 contains the posterior medians of ρ from the cash-flow-only estimations. Second, the time variation in the volatility of the long-run risk innovation, σ_{h_x}, also increases, reflecting the information in asset prices about growth uncertainty. Third, the estimate of φ_x drops from 0.435 to 0.232, which reduces the model-implied predictability of consumption growth by the price-dividend ratio and brings it more in line with the data. Finally, the estimate of σ increases somewhat from .0026 to .0032 to explain the highly volatile asset prices data.

[13]Results from the post-1959 sample with asset prices are virtually identical to the results from the post-1930 sample. For this reason, they are not plotted separately in Figure 3.

Figure 4: Smoothed States

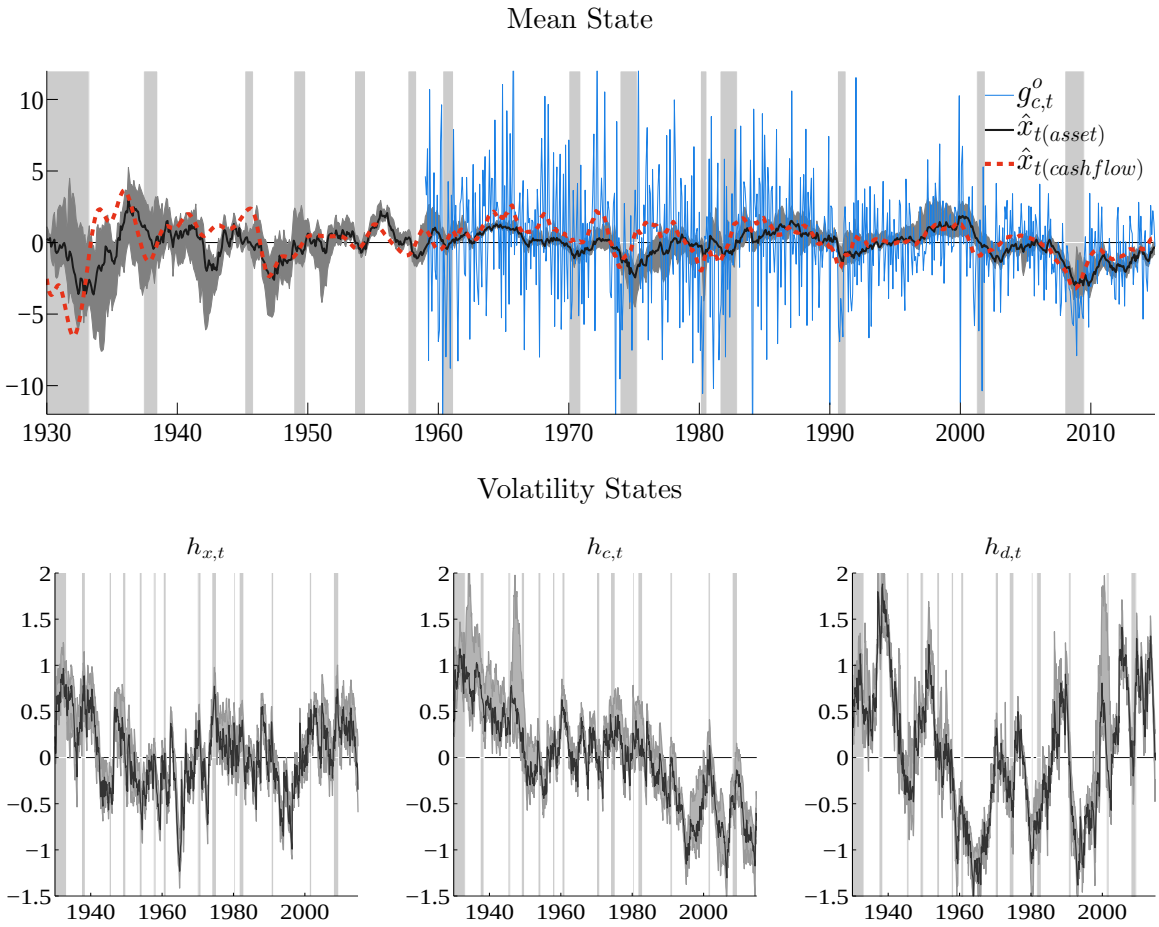

Notes: Black lines represent posterior medians of smoothed states and gray-shaded areas correspond to 90% credible intervals. Shaded bars indicate NBER recession dates. In the top panel, we overlay the smoothed state x_t obtained from the estimation without asset prices (red dashed line) and monthly consumption growth data (blue solid line).

Overall, the information from the market returns and risk-free rate reduces the posterior uncertainty about the cash flow parameters and strengthens the evidence in favor of a time-varying conditional mean of cash flow growth rates as well as time variation in the volatility components. Table 5 also provides the estimated preference parameters. The IES is estimated above 1 with a relatively tight credible band, while risk aversion is estimated at 8.6.

Smoothed Mean and Volatility States. Figure 4 depicts smoothed estimates of the predictable growth component x_t. Because the estimate of x_t is, to a large extent, determined by the time path of consumption, the 90% credible bands are much wider prior to 1960, when only annual consumption growth data were used in the estimation. Post 1959, x_t tends to fall in recessions

Table 6: Marginal Data Densities for Consumption Growth Model

Estimation	Fixed ρ					Estimated ρ
Sample	0.90	0.94	0.95	0.97	0.99	
1959-2014	2925.9	2935.9	2935.5	2934.8	2927.5	2930.1 ($\hat{\rho} = 0.95$)
1930-2014	2912.7	2914.2	2913.3	2912.1	2909.3	2909.9 ($\hat{\rho} = 0.94$)

Notes: We estimate the consumption-only model (11) conditional on various choices of ρ ("Fixed ρ") and compute marginal data densities. We also report the marginal data densities for the estimated values of ρ ("Estimated ρ") based on the posterior mean estimates (in parentheses) from Table 3.

(indicated by the shaded bars in Figure 4), but periods of falling x_t also occur during expansions. We overlay the smoothed estimate of x_t obtained from the estimation without asset price data (see Section 3.2). It is very important to note that the two estimates are similar, which highlights that x_t is, in fact, detectable based on cash flow data only. We also depict the monthly consumption growth data post 1959, which confirms that x_t indeed captures low-frequency movements in consumption growth.

The smoothed volatility processes are plotted in Figure 4. Recall that our model has three independent volatility processes, $h_{c,t}$, $h_{d,t}$, and $h_{x,t}$, associated with the innovations to consumption growth, dividend growth, and the predictable component, respectively. The most notable feature of $h_{c,t}$ is that it captures a drop in consumption growth volatility that occurred between 1930 and 1960. In magnitude, this drop in volatility is much larger than a subsequent decrease around 1984, the year typically associated with the Great Moderation. The stochastic volatility process for dividend growth shows a drop around 1955, but it also features an increase in volatility starting in 2000, which is not apparent in $h_{c,t}$. Overall, the smoothed $h_{d,t}$ seems to exhibit more medium- and high-frequency movements than $h_{c,t}$. Finally, the volatility of the persistent component, $h_{x,t}$, exhibits substantial fluctuations over our sample period, and it tends to peak during NBER recessions.

Misspecification Test. Comparing the estimates of ρ from Table 4 based on cash flow data only to the estimate obtained in Table 5 by estimating the LRR model based on cash flow and asset return data, we observed that the posterior mean increases from 0.94 and 0.95, respectively, to 0.99 once asset returns are included. To assess the extent to which the increase in ρ leads to a decrease in fit of the consumption growth process, we re-estimate model (11) conditional on various choices of ρ between 0.90 and 0.99 and re-compute the marginal data density for consumption growth. The results are summarized in Table 6. The key finding is that the drop in the marginal data density by changing ρ from $\hat{\rho}$ to 0.99 is small, indicating that there essentially is no tension between the

Figure 5: Model-Implied Risk-Free Rate

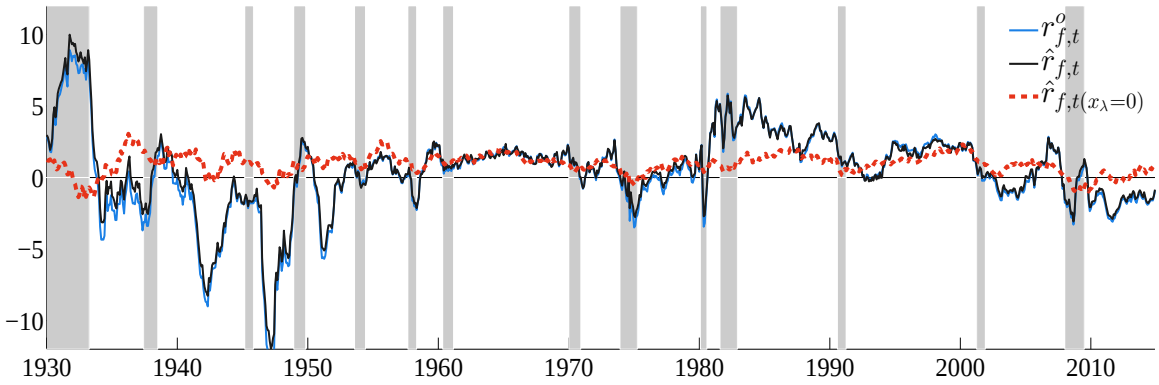

Notes: Blue line depicts the actual risk-free rate, and black line depicts the smoothed, model-implied risk-free rate without measurement errors. Red dashed line depicts the model-implied risk-free rate with $x_{\lambda,t} = 0$.

parameter estimates obtained with and without asset prices.[14]

5.3 Asset Pricing Implications

Risk-Free Rate Estimate and Preference Shock. Figure 5 overlays the actual risk-free rate, which is assumed to be subject to measurement errors, and the smoothed "true" or model-implied risk-free rate. We find that the measurement errors are fairly small. To highlight the importance of the preference shock, we also plot a counterfactual risk-free rate that would prevail in the absence of λ_t. It turns out, that ex-post much of the risk-free rate fluctuations are explained by the preference shock. In the absence of the preference shock the process for the expected stochastic discount factor implied by the predictable component of cash flow growth and the stochastic volatilities is too smooth relative to the observed risk-free rate. The preference shock can generate additional fluctuations in the expected discount factor without having a significant impact on asset returns (as we will see below).

Determinants of the Equity Risk Premium. Figure 6 depicts the contribution of short-run risk, $\sigma^2_{c,t}$, the long-run growth risk, $\sigma^2_{x,t}$, the preference risk, σ^2_λ, and the volatility risks, $\sigma^2_{w_c}$ and $\sigma^2_{w_x}$, to the risk premium; see Equation (15). We compute βs and λs based on the median posterior parameter estimates and multiply them by the median volatility state estimates to construct the risk premium. The total (annualized) equity risk premium is around 8.2%.[15] The two major sources

[14] Marginal data densities include a penalty for model dimensionality. For this reason the values with fixed $\rho = \hat{\rho}$ are slightly larger than the ones reported in the "Estimated ρ" column.

[15] The gross equity premium $\mathbb{E}[r_{m,t+1} - r_{f,t}] + 1/2\sigma^2_{r_m} \approx 0.062 + 0.5 * 0.22^2 - 0.06 = 8.2\%$.

Figure 6: Decomposition of the Equity Risk Premium

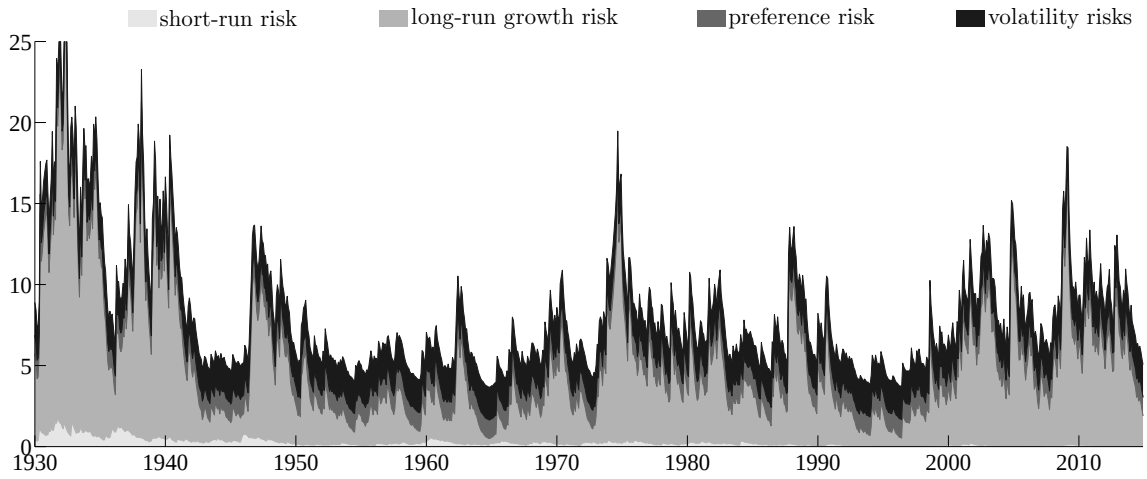

Notes: We provide the decomposition of the risk premium (15). We compute βs and λs based on the median posterior parameter estimates and multiply with the median volatility state estimates $\hat{\sigma}^2_{c,t}$ and $\hat{\sigma}^2_{x,t}$ to construct the model-implied risk premium. On average, the risk premium is accounted for by the short-run risk (0.25%), long-run growth risk (4.87%), preference risk (1.14%), and volatility risk (2.0%), respectively. Put together, the total in-sample market risk premium (annualized) is around 8.2%.

of the risk premium are the long-run growth risk and the volatility risks and when combined they account for 83% of the risk premium. More specifically, the 8.2% equity premium can be decomposed as follows. On average, the long-run growth risk generates a premium of 4.9%, the volatility risks account for 2.0%, the preference shock generates 1.1%, and the short-run volatility risk contributes 0.3%.

Determinants of Asset Price Volatility. Figure 7 depicts the contribution of the variation in growth prospects, x_t, the preference shock, $x_{\lambda,t}$, and the conditional variability of growth prospects, $\sigma_{x,t}$, to asset price volatility. We generate counterfactual volatilities by shutting down the estimated x_t, $x_{\lambda,t}$, and $\sigma_{x,t}$ processes, respectively. The ratios of the counterfactual and the actual volatilities measure the contribution of the non-omitted risk factors. We subtract this ratio from 1 to obtain the relative contribution of the omitted risk factor shown in Figure 7. Because the volatilities are time-varying, so is their relative contribution to asset price volatility.

While the preference shocks are important for the risk-free rate, they contribute very little to the variance of the price-dividend ratio and the market return. The figure shows that most of the variability of the price-dividend ratio is, in equal parts, due to the variation in x_t and $\sigma_{x,t}$. We formally show in the Online Appendix that the risk premium on the market return is barely affected by the preference shocks and consequently its variation is almost entirely attributable to the time

Figure 7: Variance Decomposition for Market Returns and Risk-Free Rate

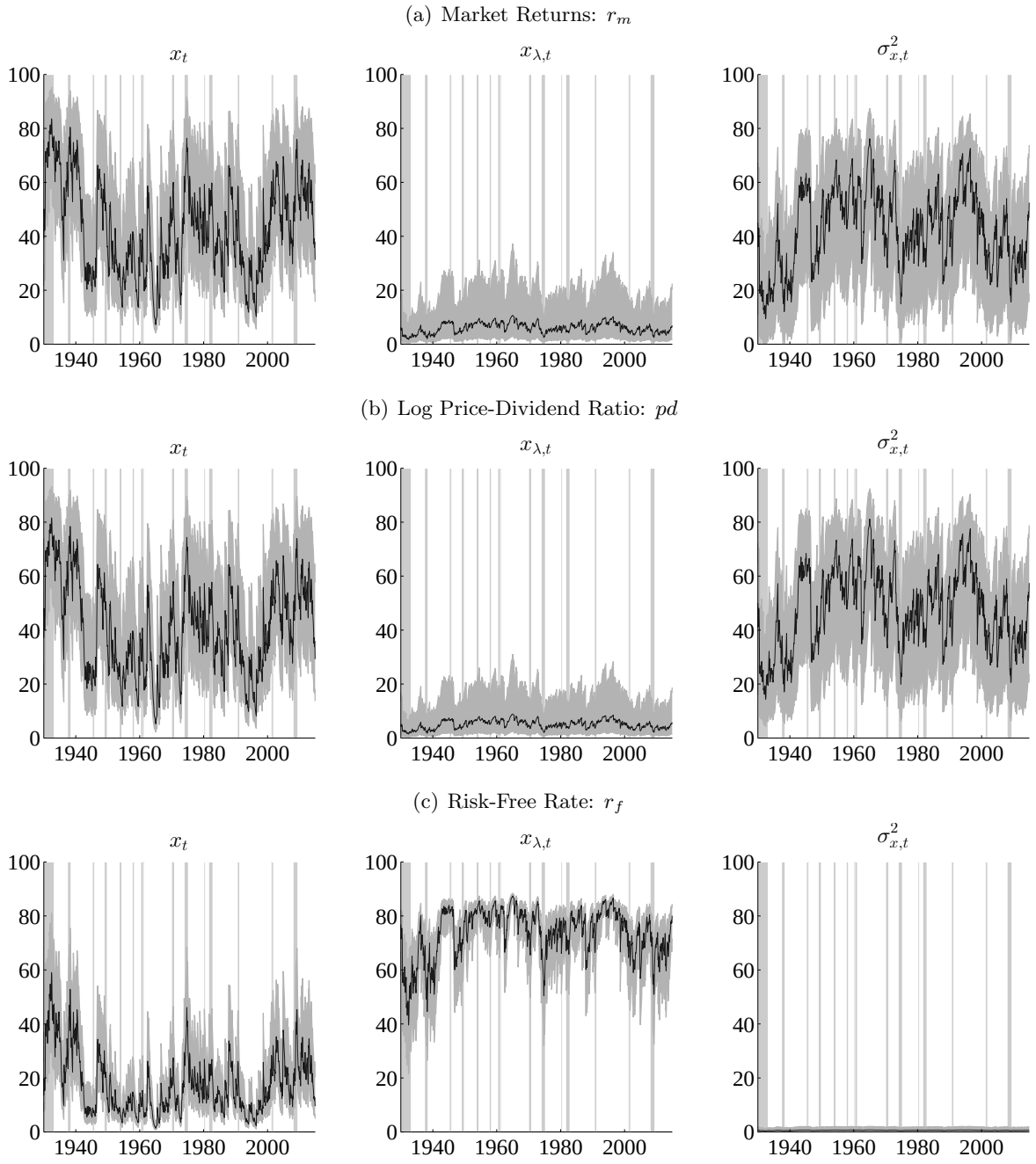

Notes: Fraction of volatility fluctuations (in percent) in the market returns, the price-dividend ratio, and the risk-free rate that is due to x_t, $x_{\lambda,t}$, and $\sigma^2_{x,t}$, respectively. We do not present the graphs for $\sigma^2_{c,t}, \sigma^2_{d,t}$ since their time-varying shares are less than 1% on average. See the main text for computational details.

variation in the stochastic volatility $\sigma^2_{x,t}$ and the growth prospect x_t. The remaining risk factors $\sigma^2_{c,t}$ and $\sigma^2_{d,t}$ have negligible effects (less than 1% on average) on asset price volatilities. However, in our likelihood-based estimation they are very important for tracking the consumption and dividend growth data.

We assumed that in our endowment economy the preference shock is uncorrelated with cash flows. In a production economy this assumption will typically not be satisfied. Stochastic fluctuations in the discount factor generate fluctuations in consumption and investment, which in turn affect cash flows. To assess whether our assumption of uncorrelated shocks is contradicted by the data, we computed the correlation between the smoothed preference shock innovations $\eta_{\lambda,t}$ and the cash flow innovations $\eta_{c,t}$ and $\eta_{x,t}$. We can do so for every parameter draw Θ^s from the posterior distribution. The 90% posterior predictive intervals range from -0.09 to 0.03 for the correlation between $\eta_{\lambda,t}$ and $\eta_{c,t}$ and from 0 to 0.2 for the correlation between $\eta_{\lambda,t}$ and $\eta_{x,t}$. Based on these results we conclude that there is no strong evidence that contradicts the assumption of uncorrelated preference shocks.

Matching Asset Price Moments. While asset pricing moments implicitly enter the likelihood function of our state-space model, it is instructive to examine the extent to which sample moments implied by the estimated state-space model mimic the sample moments computed from our actual data set. To do so, we report percentiles of the posterior predictive distribution for various sample moments based on simulations from the posterior distribution of the same length as the data.[16] While the posterior predictive distribution captures both parameter and sampling (or shock) uncertainty, we confirmed through simulation with fixed parameters that the effect of parameter uncertainty is an order of magnitude smaller than the sampling uncertainty.

Results are summarized in Table 7. Means and standard deviations refer to annualized asset prices. We first focus on the results from estimating the full model based on cash flow data and asset returns (full model estimation). It is noteworthy that all of the "actual" sample moments are within the 5th and the 95th percentile of the corresponding posterior predictive distribution.[17] The model generates a sizable mean log market return with median value of 6.2%, and a sizeable equity risk premium with a median value of about 8.2%. Consistent with the data, the model's return variability is about 20%. The high volatility of the market returns translates into a large variability of the sample moments. The autocorrelation of the market return is very small. The

[16] This is called a posterior predictive check; see Geweke (2005) for a textbook treatment. Specifically, the percentiles are obtained using the following simulation: draw parameters Θ^s from the posterior distribution; for each Θ^s simulate a trajectory Y^s (same number of observations as in the actual sample) and compute the sample statistics $\mathcal{S}(Y^s)$ of interest.

[17] Although not reported in the table this is also the case for the mean, standard deviation and first autocorrelation moments of consumption and dividend growth.

Table 7: Asset Return Moments

		Parameter Estimates are Based On					
	Data	Cash Flows & Asset Returns			Cash Flows Only		
		5%	50%	95%	5%	50%	95%
Mean (r_m)	6.06	3.18	6.20	10.53	1.08	3.53	5.92
StdDev (r_m)	19.8	11.7	22.7	52.4	10.1	15.0	27.3
AC1 (r_m)	-0.01	-0.27	-0.05	0.19	-0.30	-0.03	0.20
Corr ($\Delta c, r_m$)	0.11	-0.10	0.11	0.28	-0.08	0.12	0.34
Mean (r_f)	0.37	-0.34	0.60	1.43	1.48	1.83	2.10
StdDev (r_f)	2.85	1.81	2.29	2.90	0.64	0.88	1.28
AC1 (r_f)	0.64	0.33	0.53	0.66	0.23	0.44	0.63
Mean (pd)	3.40	2.58	3.14	3.41	3.70	3.78	3.83
StdDev (pd)	0.45	0.14	0.31	0.98	0.09	0.15	0.27
AC1 (pd)	0.87	0.55	0.79	0.90	0.23	0.53	0.73

Notes: We present descriptive statistics for log returns of the aggregate stock market (r_m), its correlation with consumption growth (Δc), the log risk-free rate (r_f), and the log price-dividend ratio (pd). We report means (Mean), standard deviations (StdDev), first-order sample autocorrelations (AC1), and correlations (Corr). Market returns, the risk-free rate, and the price-dividend ratio refer to 12-month averages (in percent). Computing asset pricing implications for the cash-flow-only estimates requires calibration of the preference parameters. We set δ, ψ, γ to median posterior estimates from Table 5.

model, partly through the preference shocks, generates a risk-free rate that reproduces the strong positive serial correlation found in the data. As in the data, the model generates both a highly variable and persistent price-dividend ratio. It is particularly noteworthy that the median and 95th percentile of the price-dividend volatility distribution are significantly larger than in other LRR calibrated models with Gaussian shocks. This feature owes in part to the fact that the models contain three volatility components with underlying log-volatility dynamics, thus accommodating some non-Gaussian features.

In Section 5.2 we noted that the parameter estimates for the cash flow processes change a bit once asset pricing data are included. To assess the economic implications of the parameter differentials we conduct the following experiment. We combine the posterior median estimates of the preference parameters from the full estimation with the cash flow process parameter estimates reported in Table 4 (1930-2014 sample). Because the cash-flow-only model was estimated without the preference

shock $x_{\lambda,t}$ and the third volatility process $\sigma^2_{x,t}$ we drop these two state-variables from the pricing equations when re-computing the asset pricing implications of the LRR model. The results are summarized in the last three columns of Table 7.

Even without the information content of asset prices or of the preference shocks, the cash-flow-only estimates are able to generate credible bands that are consistent with many moments of the data.[18] The median market return and its volatility are now lower relative to the full estimation results, yet their 95% percentiles are still as high as 5.9% and 27% respectively (with a gross equity premium of about 3%). Note that these numbers provide a conservative picture for the performance of the cash-flow-only estimates because the preference parameters are based on the estimation of the full model. One noticeable difference between the cash-flow-only estimates and the full-model estimates is in the risk free rate moments. Unlike the specification based on the cash-flow-only estimates, the full model incorporates the preference shock which reduces the mean risk free rate and increases its volatility. Finally, the cash-flow-only estimates generate a price-dividend ratio that is not as volatile or persistent as the one in the data. The increased persistence in the full estimation leads to a more volatile and persistent model price-dividend ratio.

Consumption Growth and Excess Return Predictability. One aspect of the data that is often discussed in the context of asset pricing models — and in particular, in the context of models featuring long-run risks — is the low predictability of future consumption growth by the current price-dividend ratio. Another key issue in the asset pricing literature is return predictability by the price-dividend ratio (e.g., Hodrick (1992)).

We consider two types of predictability checks: multivariate and univariate. In the model, and possibly in the data, the price-dividend ratio reflects multiple state variables. Consequently, a VAR-based predictive regression is a natural starting point. As in Bansal, Kiku, and Yaron (2012) we estimate a first-order VAR that includes consumption growth, the price-dividend ratio, the real risk-free rate, and the market return. Based on the estimated VAR coefficients we compute R^2's for cumulative H-step-ahead consumption growth and excess returns:

$$\sum_{h=1}^{H} \Delta c_{t+h} \quad \text{and} \quad \sum_{h=1}^{H} (r_{m,t+h} - r_{f,t+h-1}).$$

While the VAR-based predictive checks are appealing from a theoretical perspective, much of the empirical literature focuses on R^2's from univariate predictive regressions using the price-dividend ratio as the only regressor.

[18] Chen, Dou, and Kogan (2015) formalize this comparison by developing a measure of model fragility, roughly speaking based on the discrepancy between the posterior medians obtained under the cash-flow-only estimation and the estimation with asset returns.

The results are presented as posterior predictive checks, similar to those in Table 7, but now depicted graphically in Figure 9. The sample statistics considered are the R^2 values obtained from the two regressions. The top and bottom ends of the boxes correspond to the 5th and 95th percentiles, respectively, of the posterior predictive distribution, and the horizontal bars signify the medians. To facilitate meaningful comparisons of the predictive regressions across models (to be described below), we condition the predictive analysis on the posterior median estimates of the LRR model. This is innocuous because, as mentioned previously, the contribution of parameter uncertainty to the variability of the posterior predictive distribution is small. Thus, the predictive intervals reflect the fact that we are repeatedly generating data from the model and computing a sample statistic for each of these simulated trajectories. Finally, the small squares correspond to statistics computed from "actual" U.S. data.

The top and bottom left panels of Figure 9 depict results for the VAR-based predictability regressions. The first thing to note is that, with multiple predictive variables, consumption growth is *highly* predictable in the data. For instance, at the one-year horizon the R^2 is about 52% (see also Bansal, Kiku, Shaliastovich, and Yaron (2014)). While the predictability diminishes over time, it is still nontrivial with an R^2 of 12% at the 10-year horizon. The key finding is that the model-implied VAR-based estimates has predictability implications that are very similar to the ones observed in the actual data. At the one-year horizon the median of the model-implied R^2 is somewhat lower than its data estimate, whereas over horizons of three years or more, it is slightly larger than the data estimate. Noteworthy, in terms of excess return predictability the medians of the model-based estimates are almost perfectly aligned with the data-based estimates.

The subplots in Column 2 of Figure 9 provide the results of the univariate predictive regressions. This column is labeled "Benchmark" because, as for the VAR-based predictability checks, we simulate the LRR model with all of its five state variables: x_t, $x_{\lambda,t}$, $\sigma^2_{x,t}$, $\sigma^2_{c,t}$, and $\sigma^2_{d,t}$. As is well known, when the price-dividend ratio is used as a single regressor, it produces low R^2s for predicting consumption growth. It is less than 5% for horizons from one to eight years and reaches almost 10% at the ten-year horizon. The median R^2 values obtained from regressions on model-generated data are between 10% to 15%, slightly higher than in the actual data. However, the posterior predictive intervals range from 0 to 30% for the one-year horizon and from 0 to about 50% for horizons longer than three years. Thus, in that sense the model does well in covering the data R^2s.

The model also performs very well in terms of the univariate excess return predictability regressions. Specifically, for all horizons the median of the model-implied distribution of R^2s are quite close to actual data R^2s and the model-based credible intervals contain the R^2 obtained from the actual data. The good performance is obtained because, according to the model, the price-dividend

Figure 8: Predictability Checks

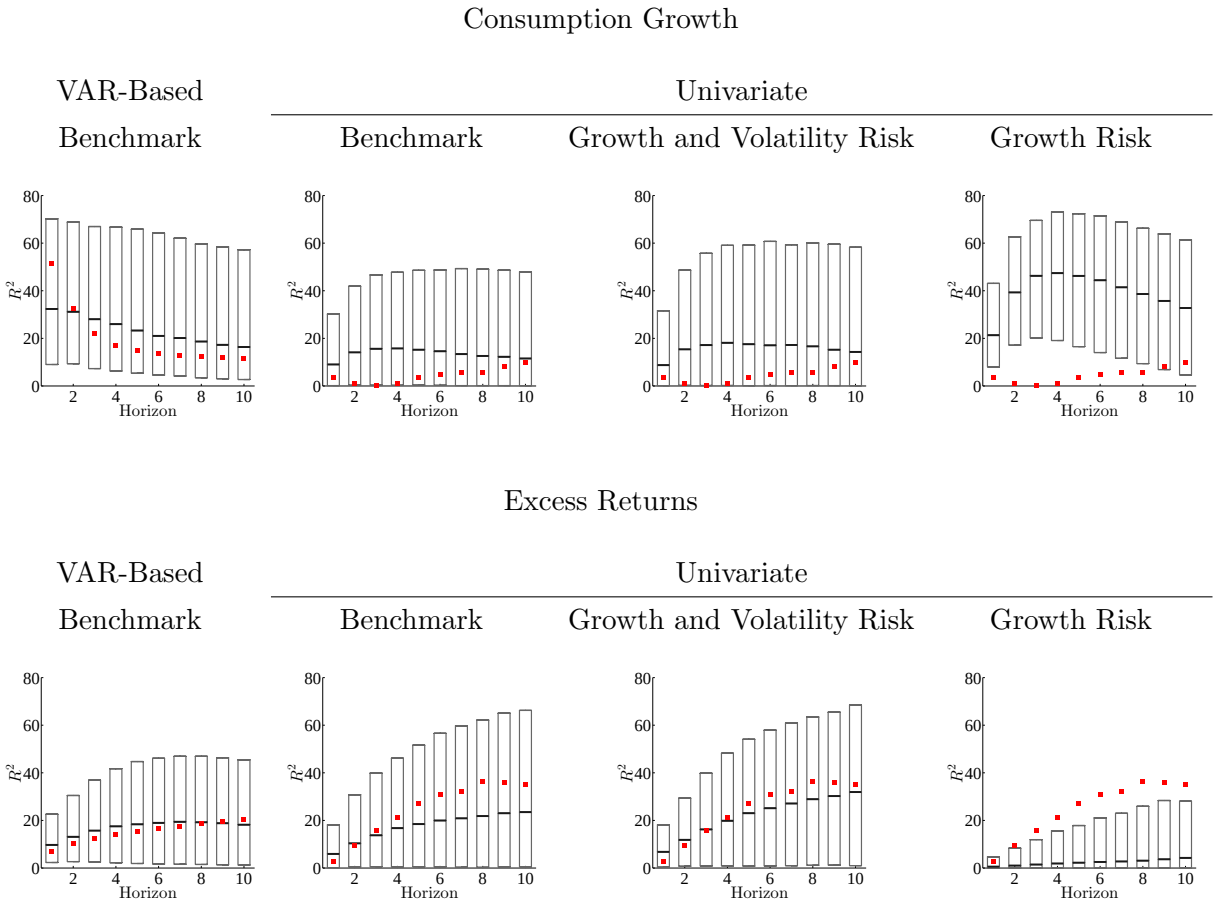

Notes: We fix the parameters at their posterior median estimates. The red squares represent R^2 values obtained from the actual data. The boxes represent 90% posterior predictive intervals and the horizontal lines represent medians. The "Benchmark" case is based on simulations with all five state variables x_t, $x_{\lambda,t}$, $\sigma^2_{x,t}$, $\sigma^2_{c,t}$, and $\sigma^2_{d,t}$; "Growth and Volatility Risk" is based on x_t and $\sigma^2_{x,t}$ only; "Growth Risk" is based on x_t only. The horizon is measured in years. The VAR-Based R^2s are constructed as in Hodrick (1992).

ratio is the most important predictor of long-horizon excess returns among the observables. Thus, the results from the univariate regressions are not very different from the VAR-based ones.

In order to understand how individual risk factors affect predictability, we proceed by simulating two restrictive model specifications that only incorporate a subset of the state variables: "Growth and Volatility Risks" includes only x_t and $\sigma^2_{x,t}$; and "Growth Risk" includes only x_t. In doing so we continue to use the posterior median parameter estimates reported in Table 5. The results for these respective specifications are given in Columns 3 and 4 of Figure 9. It is evident that the "Growth and Volatility Risk" plots are very similar to the "Benchmark" plots for both consumption and

return predictability as x_t and $\sigma^2_{x,t}$ are ultimately the key state variables driving the price-dividend ratio.[19]

The credible intervals for the "Growth Risk" predictive regressions do not include the actual data estimates. This specification generates too much consumption predictability and thereby highlights that the volatility shocks play an important role in lowering the model-implied predictability to a more realistic level. Because the time variation in risk premia in the model is exclusively driven by stochastic volatilities, the "Growth Risk" specification, which excludes all three stochastic volatility processes, generates relatively small credible intervals for the excess return predictability. These credible intervals are entirely driven by finite sample properties of the simulations. Because in the model excess returns do not load on x_t, the R^2s will converge to zero as the simulation sample length goes to infinity.

While our model passes the predictive checks, the credible intervals depicted in Figure 9 are wide, meaning that the sampling distribution of the R^2 measures is highly variable. The diffuse and skewed sampling distributions of the R^2 statistics are caused by various non-standard features of predictive regressions. Due to overlapping time periods, residuals are typically serially correlated and lagged residuals may be correlated with the predictor. Moreover, the persistent component of the dependent variable (consumption growth or excess returns) is dominated by *iid* shocks and the right-hand-side regressor (price-dividend ratio) is highly persistent – a feature that can render the predictive regressions spurious (see Hodrick (1992) and Stambaugh (1999)).[20]

Dividend Growth Predictability. Cochrane (2011) argues that there is very little dividend growth predictability at all horizons. This view is based on a univariate regression with the price-dividend ratio as a predictor of future dividend growth. The data feature modest predictability, with an R^2 in the range of 4% to 9%, depicted by the red squares in the left panel of Figure 9. However, dividend growth is found to be highly predictable both at short and long horizons, once additional predictors are included in a VAR based predictive regression, with adjusted R^2s as large as 35% at the 10-year horizon (see Column 2 of Figure 9).[21] Importantly, in both the univariate

[19]The R^2s in the "Growth and Volatility Risks" are slightly larger than the "Benchmark" for the consumption predictability regressions. This follows because the price-dividend ratio no longer fluctuates in response to preference shocks, which have no bearing on consumption growth.

[20]Valkanov (2003) derived an asymptotic distribution of the R^2 under the assumption that the regressor follows a local-to-unity process. He shows that the goodness-of-fit measure converges to a random limit as the sample size increases. More recently, Bauer and Hamilton (2015) studied the sampling distribution of R^2 measures in predictive regressions for bond returns, which exhibit similar distortions.

[21]This evidence is consistent with Lettau and Ludvigson (2005), Koijen and van Binsbergen (2010), and Jagannathan and Liu (2016) who report R^2 values from a VAR-based regression that range from 10% to 40%.

Figure 9: Dividend Growth Predictability and Dividend Yield Variance Decomposition

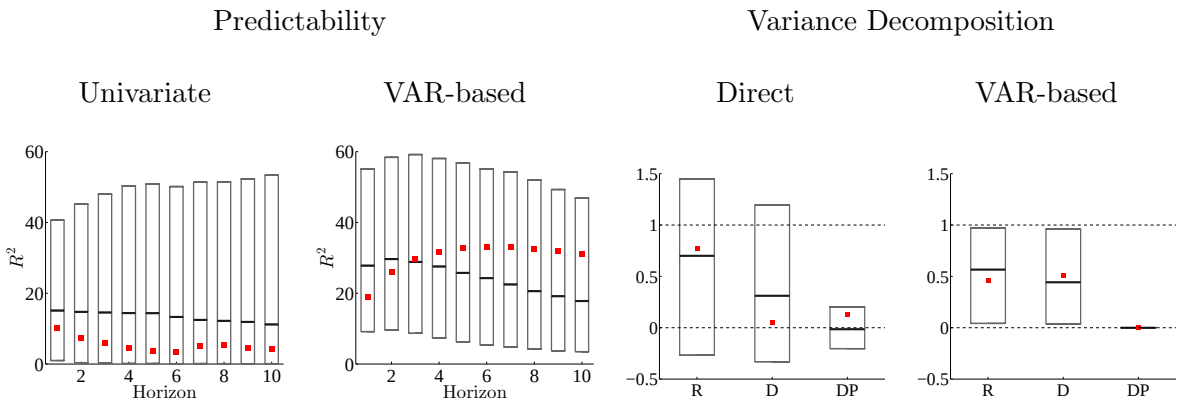

Notes: (Predictability) We fix the parameters at their posterior median estimates and simulate the data. The horizon is measured in years. We run a univariate regression with the price-dividend ratio as predictor of future dividend growth. For the multivariate regression, we consider a first-order VAR that includes consumption growth, dividend growth, the price-dividend ratio, and the real risk-free rate. Based on the estimated coefficients we compute R^2's for cumulative H-step-ahead dividend growth. The red squares represent R^2 values obtained from the actual data. The boxes represent 90% posterior predictive intervals and the horizontal lines represent medians. The VAR-based R^2s are constructed as in Hodrick (1992). (Variance Decomposition, Direct) We regress 15-year ex post returns, dividend growth, and dividend yield, respectively, on a constant term and the dividend yield. (Variance Decomposition, VAR-based) We infer long-run coefficients ($k \to \infty$) from 1-year coefficients of the same VAR used for the predictability analysis. Using the Campbell-Shiller approximation, the fractions of dividend yield variation attributed to each source are provided as $1 \approx \frac{Cov(dp_t, \sum_{j=1}^{k} \rho^{j-1} r_{t+j})}{Var(dp_t)} - \frac{Cov(dp_t, \sum_{j=1}^{k} \rho^{j-1} \Delta d_{t+j})}{Var(dp_t)} + \frac{\rho^k Cov(dp_t, dp_{t+k})}{Var(dp_t)}$. These components are marked as R, D, and DP respectively.

and VAR-based predictive regressions, the model implications for dividend growth predictability line up with the data and cover the data R^2s.

The strong evidence for dividend growth predictability has important implications for the variability of the log dividend yield dp_t. Based on the Campbell and Shiller (1988a) approximate present value identity it follows that

$$dp_t \approx \sum_{j=1}^{k} \rho^{j-1} r_{t+j} - \sum_{j=1}^{k} \rho^{j-1} \Delta d_{t+j} + \rho^k dp_{t+k}, \tag{19}$$

where ρ is an approximation constant based on the average dividend yield. Multiplying both sides of (19) by the log dividend yield and taking expectations implies that the variance of the current dividend yield can be attributed to its covariance with expected future returns, dividend growth rates, and the expected future dividend yield, respectively, marked as "R", "D", and "DP" in Figure 9 (see figure notes for details). As k approaches infinity, the dividend yield variability is explained completely by covariation with expected returns and cash flow growth. We compute the fraction of variability explained by the three covariances via "Direct" regression (setting k equal

Figure 10: Correlation between Market Return and Growth Rates of Fundamentals

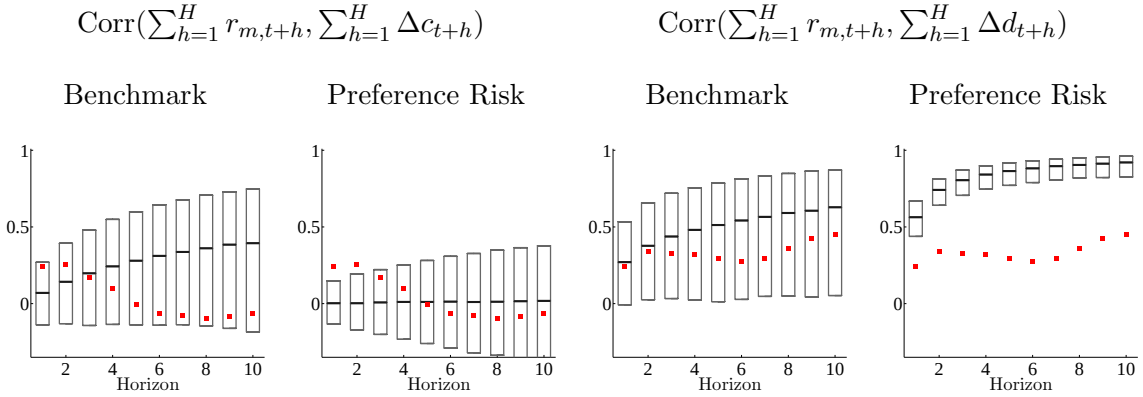

Notes: We fix the parameters at their posterior median estimates. The "Benchmark" case is based on simulations with all five state variables x_t, $x_{\lambda,t}$, $\sigma^2_{x,t}$, $\sigma^2_{c,t}$, and $\sigma^2_{d,t}$; "Preference Risk" is based on $x_{\lambda,t}$ only.

to 15 years and separately regressing the "R", "D", and "DP" components on the dividend yield) and "VAR-based" regression (inferring the $k = \infty$ decomposition from the coefficients of a VAR estimated based on annual data). The estimates based on the direct regressions attribute much of the variation in dividend yield to variation in discount rates (although not entirely), whereas the point estimates of the VAR attribute about half of the variation to discount rates and the other to dividend growth. Again, it is important to note that in both cases the model credible intervals contain the data point estimates. Moreover, in both cases the credible intervals around the point estimates are consistent with a view in which a large portion (about half) of the dividend yield variability is driven by cash flows.

Long-Horizon Correlations. One additional feature of the data is the long horizon correlation between consumption growth (dividend growth) and returns –that is the H-th horizon correlation $corr(\sum_{h=1}^{H} r_{m,t+h}, \sum_{h=1}^{H} \Delta c_{t+h})$. Our model performs well along this dimension, which is presented in Figure 10. Several important points emerge. In the "Benchmark" specification, the 10-year consumption growth and 10-year return have a correlation of 0.3, but with a very wide credible interval that encompass -0.2 to 0.7, which importantly contains the data estimate. The analogous correlation credible interval for dividend growth ranges from 0 to 0.8, with the data at 0.4 and again very close to the model median estimate. It is also noteworthy that these correlation features are primarily driven by "Growth and Volatility Risks." Although not reported, the plots based on the "Growth and Volatility Risks" specification are very similar to the "Benchmark" specification. Albuquerque, Eichenbaum, Luo, and Rebelo (2016) highlight that preference shocks improve the LRR model-performance for these long horizon correlations. The "Preference Risk" subplots provide the

correlations when all shocks except $x_{\lambda,t}$ are shutdown. These plots show that the preference shocks improve fit by generating lower credible intervals for consumption, yet deteriorate fit by generating way too large long horizon correlations for dividends.

6 Conclusion

We developed a non-linear Bayesian state-space model that utilizes mixed frequency data to study the time series dynamics of consumption and its implications for asset pricing. We show that after accounting for monthly measurement errors there is strong evidence for both a small persistent predictable component as well as a stochastic volatility component in consumption growth. Importantly, this evidence emerges when the estimation uses only consumption data, and is reinforced and sharpened when the estimation uses the joint dynamics of consumption, dividends, and asset return data. The estimation identifies three volatility processes which control the short run dynamics, variation in economy-wide trend, and independent dividend dynamics, respectively. The model is able to successfully capture many asset pricing moments and improve upon key predictability moments of previous LRR models.

References

Albuquerque, R., M. Eichenbaum, V. Luo, and S. Rebelo (2016): "Valuation Risk and Asset Pricing," *Journal of Finance, forthcoming.*

Amir-Ahmadi, P., C. Matthes, and M.-C. Wang (2016): "Drifts and Volatilities under Measurement Error: Assessing Monetary Policy Shocks over the Last Century," *Quantitative Economics, forthcoming.*

Andreasen, M. (2010): "Stochastic Volatility and DSGE Models," *Economics Letters*, 108, 7–9.

Andrieu, C., A. Doucet, and R. Holenstein (2010): "Particle Markov Chain Monte Carlo Methods (with Discussion)," *Journal of the Royal Statistical Society, Series B*, 72, 1–33.

Aruoba, S., F. Diebold, and C. Scotti (2009): "Real-Time Measurement of Business Conditions," *Journal of Business and Economic Statistics*, 27(4), 417–427.

Bansal, R., A. Gallant, and G. Tauchen (2007): "Rational Pessimism, Rational Exuberance, and Asset Pricing Models," *Review of Economic Studies*, 74, 1005–1033.

Bansal, R., V. Khatacharian, and A. Yaron (2005): "Interpretable Asset Markets?," *European Economic Review*, 49, 531–560.

Bansal, R., D. Kiku, I. Shaliastovich, and A. Yaron (2014): "Volatility, the Macroeconomy and Asset Prices," *Journal of Finance*, 69, 2471–2511.

Bansal, R., D. Kiku, and A. Yaron (2012): "An Empirical Evaluation of the Long-Run Risks Model for Asset Prices," *Critical Finance Review*, 1, 183–221.

——— (2014): "Risks for the Long Run: Estimation with Time Aggregation," Manuscript, University of Pennsylvania and Duke University.

Bansal, R., and A. Yaron (2004): "Risks For the Long Run: A Potential Resolution of Asset Pricing Puzzles," *Journal of Finance*, 59, 1481–1509.

Barro, R. (2009): "Rare Disasters, Asset Prices, and Welfare Costs," *American Economic Review*, 99, 243–264.

Bauer, M., and J. Hamilton (2015): "Robust Bond Risk Premia," Federal Reserve Bank of San Francisco Working Paper 2015-15.

Beeler, J., and J. Campbell (2012): "The Long-Run Risks Model and Aggregate Asset Prices: An Empirical Assessment," *Critical Finance Review*, 1, 141–182.

Bloom, N. (2009): "The Impact of Uncertainty Shocks," *Econometrica*, 77, 623–685.

Campbell, J., and J. Cochrane (1999): "By Force of Habit: A Consumption-Based Explanation of Aggregate Stock Market Behavior," *Journal of Political Economy*, 107, 205–251.

Campbell, J., and R. Shiller (1988a): "The Dividend-Price Ratio and Expectations of Future Dividends and Discount Factors," *Review of Financial Studies*, 1, 195–227.

——— (1988b): "Stock Prices, Earnings, and Expected Dividends," *Journal of Finance*, 43, 661–676.

Carter, C. K., and R. Kohn (1994): "On Gibbs Sampling for State Space Models," *Biometrika*, 81(3), 541–553.

Chen, H., W. D. Dou, and L. Kogan (2015): "Measuring the "Dark Matter" in Asset Pricing Models," *Manuscript, MIT*.

Chen, R., and J. Liu (2000): "Mixture Kalman Filters," *Journal of the Royal Statistical Society Series B*, 62, 493–508.

Chernov, M., R. Gallant, E. Ghysels, and G. Tauchen (2003): "Alternative Models for Stock Price Dynamics," *Journal of Econometrics*, 116, 225–257.

Cochrane, J. (2011): "Presidential Address: Discount Rates," *Journal of Finance*, 66(4), 1047–1108.

Creal, D. D., and J. C. Wu (2015): "Bond Risk Premia in Consumption-based Models," *Manuscript, Chicago Booth*.

Doh, T., and S. Wu (2015): "Cash Flow and Risk Premium Dynamics in an Equilibrium Asset Pricing Model with Recursive Preferences," *FRB Kansas City Research Working Paper*, 15-12.

Drost, F., and T. Nijman (1993): "Temporal Aggregation of Garch Processes," *Econometrica*, 61, 909–927.

Epstein, L., and S. Zin (1989): "Substitution, Risk Aversion and the Temporal Behavior of Consumption and Asset Returns: A Theoretical Framework," *Econometrica*, 57, 937–969.

Fernández-Villaverde, J., and J. F. Rubio-Ramírez (2007): "Estimating Macroeconomic Models: A Likelihood Approach," *Review of Economic Studies*, 74(4), 1059–1087.

Fernández-Villaverde, J., and J. F. Rubio-Ramírez (2011): "Macroeconomics and Volatility: Data, Models, and Estimation," in *Advances in Economics and Econometrics: Theory and Applications, Tenth World Congress of the Econometric Society*, ed. by D. Acemoglu, M. Arellano, and E. Deckel. Cambridge University Press.

Geweke, J. (2005): *Contemporary Bayesian Econometrics and Statistics*. New Jersey: John Wiley & Sons.

Gourio, F. (2012): "Disaster Risk and Business Cycles," *American Economic Review*, 102(6), 2734?2766.

Hall, R. (1978): "Stochastic Implications of the Life Cycle-Permanent Income Hypothesis: Theory and Evidence," *Journal of Political Economy*, 86(6), 971?986.

Hansen, L. (2007): "Beliefs, Doubts and Learning: Valuing Macroeconomic Risk," *American Economic Review*, 97(2), 1–30.

Hansen, L., and T. Sargent (2007): *Robustness*. Princeton University Press.

Hansen, L. P., J. C. Heaton, and N. Li (2008): "Consumption Strikes Back? Measuring Long-Run Risk," *Journal of Political Economy*, 116(2), 260–302.

Harvey, A. (1989): *Forecasting, Structural Time Series Models and the Kalman Filter*. Cambridge University Press.

Herbst, E., and F. Schorfheide (2015): *Bayesian Estimation of DSGE Models*. Princeton University Press.

Hodrick, R. (1992): "Dividend Yields and Expected Stock Returns: Alternative Procedures for Inference and Measurement," *Review of Financial Studies*, 5, 357–386.

Jagannathan, R., and B. Liu (2016): "Dividend Dynamics, Learning, and Expected Stock Index Returns," Manuscript, Northwestern University.

Johannes, M., L. Lochstoer, and Y. Mou (2016): "Learning about Consumption Dynamics," *Journal of Finance, forthcoming*.

Kim, S., N. Shephard, and S. Chib (1998): "Stochastic Volatility: Likelihood Inference and Comparison with ARCH Models," *Review of Economic Studies*, 65, 361–393.

Koijen, R., and J. van Binsbergen (2010): "Predictive Regressions: A Present-Value Approach," *Journal of Finance*, 65(4), 1439–1471.

Lettau, M., and S. Ludvigson (2005): "Expected Returns and Expected Dividend Growth," *Journal of Financial Economics*, 76(3), 583–626.

Lucas, R. (1978): "Asset Prices in an Exchange Economy," *Econometrica*, 46(6), 1429–1445.

Mariano, R., and Y. Murasawa (2003): "A New Coincident Index of Business Cycles Based on Monthly and Quarterly Series," *Journal of Applied Econometrics*, 18, 427–443.

Nakamura, E., D. Sergeyev, and J. Steinsson (2015): "Growth-Rate and Uncertainty Shocks in Consumption: Cross-Country Evidence," *Manuscript, Columbia University*.

Pitt, M., and N. Shephard (1999): "Filtering via Simulation: Auxiliary Particle Filters," *Journal of the American Statistical Association*, 94, 590–599.

Romer, C. (1986): "New Estimates of Prewar Gross National Product and Unemployment," *The Journal of Economic History*, 46(2), 341–352.

Romer, C. (1989): "The Prewar Business Cycle Reconsidered: New Estimates of Gross National Product, 1869-1908," *Journal of Political Economy*, 97(1), 1–37.

Schorfheide, F., and D. Song (2015): "Real-Time Forecasting with a Mixed-Frequency VAR," *Journal of Business and Economic Statistics*, 33(3), 366–380.

Shephard, N. (2015): "Martingale Unobserved Component Models," in *Unobserved Components and Time Series Econometrics*, ed. by S. J. Koopman, and N. Shephard, pp. 218–249. Oxford University Press.

Slesnick, D. (1998): "Are Our Data Relevant to the Theory? The Case of Aggregate Consumption," *Journal of Business and Economic Statistics*, 16(1), 52–61.

Stambaugh, R. F. (1999): "Predictive Regressions," *Journal of Financial Economics*, 54, 375–421.

Valkanov, R. (2003): "Long-Horizon Regressions: Theoretical Results and Applications," *Journal of Financial Economics*, 68, 201–232.

Wilcox, D. (1992): "The Construction of the U.S. Consumption Data: Some Facts and Their Implications for Empirical Work," *American Economic Review*, 82, 922–941.

Appendix

A Data Source

A.1 Nominal PCE

We download seasonally adjusted data for nominal PCE from NIPA Tables 2.3.5 and 2.8.5. We then compute within-quarter averages of monthly observations and within-year averages of quarterly observations.

A.2 Real PCE

We use Table 2.3.3., Real Personal Consumption Expenditures by Major Type of Product, Quantity Indexes (A:1929-2014)(Q:1947:Q1-2014:Q4) to extend Table 2.3.6., Real Personal Consumption Expenditures by Major Type of Product, Chained Dollars (A:1995-2014) (Q:1995:Q1-2014:Q4). Monthly data are constructed analogously using Table 2.8.3. and Table 2.8.6.

A.3 Real Per Capita PCE: ND+S

The LRR model defines consumption as per capita consumer expenditures on nondurables and services. We download mid-month population data from NIPA Table 7.1.(A:1929-2014)(Q:1947:Q1-2014:Q4) and from Federal Reserve Bank of St. Louis' FRED database (M:1959:M1-2014:M12). We convert consumption to per capita terms.

A.4 Dividend and Market Returns Data

Data are from the Center for Research in Security Prices (CRSP). The three monthly series from CRSP are the value-weighted with-, RN_t, and without-dividend nominal returns, RX_t, of CRSP stock market indexes (NYSE/AMEX/NASDAQ/ARCA), and the CPI inflation rates, π_t. The sample period is from 1929:M1 to 2014:M12. The monthly real dividend series are constructed as in Hodrick (1992):

1. A normalized nominal value-weighted price series is produced by initializing $P_0 = 1$ and recursively setting $P_t = (1 + RX_t)P_{t-1}$.

2. A normalized nominal divided series, D_t^{Raw}, is obtained by recognizing that $D_t^{Raw} = (RN_t - RX_t)P_{t-1}$.

3. Following Robert Shiller we smooth out dividend series by aggregating 3 months values of the raw nominal dividend series $D_t = \sum_{i=0}^{2} D_{t-i}^{Raw}$ and apply the following quarterly interpolation. Here, D_t, D_{t-3}, ... is the last month of the quarter.

$$D_{t-m} = D_t - \frac{m}{3}(D_t - D_{t-3}), \quad m \in \{0, 1, 2\}. \tag{A.1}$$

4. We then compute the real dividend growth $g_{d,t}$ by subtracting the actual inflation from the interpolated nominal dividend growth

$$g_{d,t} = \log(D_t) - \log(D_{t-1}) - \pi_t. \tag{A.2}$$

   Here inflation rates are computed using the log differences of the consumer price index (CPI) from the Bureau of Labor Statistics.

Market returns, RN_{t+1}, are also converted from nominal to real terms using the CPI inflation rates and denoted by $r_{m,t+1}$.

A.5 Ex Ante Risk-Free Rate

The ex ante risk-free rate is constructed as in the online appendix of Beeler and Campbell (2012). Nominal yields to calculate risk-free rates are the CRSP Fama Risk Free Rates. Even though our model runs in monthly frequencies, we use the three-month yield because of the larger volume and higher reliability. We subtract annualized three-month inflation, $\pi_{t,t+3}$, from the nominal yield, $i_{f,t}$, to form a measure of the ex post (annualized) real three-month interest rate. The ex ante real risk-free rate, $r_{f,t}$, is constructed as a fitted value from a projection of the ex post real rate on the current nominal yield, $i_{f,t}$, and inflation over the previous year, $\pi_{t-12,t}$:

$$\begin{aligned} i_{f,t} - \pi_{t,t+3} &= \beta_0 + \beta_1 i_{f,t} + \beta_2 \pi_{t-12,t} + \varepsilon_{t+3} \\ r_{f,t} &= \hat{\beta}_0 + \hat{\beta}_1 i_{f,t} + \hat{\beta}_2 \pi_{t-12,t}. \end{aligned}$$

The ex ante real risk-free rates are available from 1929:M1 to 2014:M12.

B The Measurement-Error Model for Consumption

For expositional purposes, we assume that the accurately measured low-frequency observations are available at quarterly frequency (instead of annual frequency as in the main text). Correspondingly, we define the time subscript $t = 3(j-1)+m$, where month $m = 1, 2, 3$ and quarter $j = 1, \ldots$. We use uppercase C to denote the level of consumption and lowercase c to denote percentage deviations from some log-linearization point. Growth rates are approximated as log differences and we use a superscript o to distinguish observed from "true" values.

The measurement-error model presented in the main text can be justified by assuming that the statistical agency uses a high-frequency proxy series to determine monthly consumption growth rates. We use $Z_{3(j-1)+m}$ to denote the monthly value of the proxy series and $Z^q_{(j)}$ the quarterly aggregate. Suppose the proxy variable provides a noisy measure of monthly consumption. More specifically, we consider a multiplicative error model of the form

$$Z_{3(j-1)+m} = C_{3(j-1)+m} \exp(\epsilon_{3(j-1)+m}). \tag{A.3}$$

The interpolation is executed in two steps. In the first step we construct a series $\tilde{C}^o_{3(j-1)+m}$, and in the second step we rescale the series to ensure that the reported monthly consumption data add up to the reported quarterly consumption data within the period. In Step 1, we start from the level of consumption in quarter $j-1$, $C^q_{(j-1)}$, and define

$$\begin{aligned}
\tilde{C}^o_{3(j-1)+1} &= C^{q,o}_{(j-1)} \left(\frac{Z_{3(j-1)+1}}{Z^q_{(j-1)}} \right) \\
\tilde{C}^o_{3(j-1)+2} &= C^{q,o}_{(j-1)} \left(\frac{Z_{3(j-1)+1}}{Z^q_{(j-1)}} \right) \left(\frac{Z_{3(j-1)+2}}{Z_{3(j-1)+1}} \right) = C^{q,o}_{(j-1)} \left(\frac{Z_{3(j-1)+2}}{Z^q_{(j-1)}} \right) \\
\tilde{C}^o_{3(j-1)+3} &= C^{q,o}_{(j-1)} \left(\frac{Z_{3(j-1)+1}}{Z^q_{(j-1)}} \right) \left(\frac{Z_{3(j-1)+2}}{Z_{3(j-1)+1}} \right) \left(\frac{Z_{3(j-1)+3}}{Z_{3(j-1)+2}} \right) = C^{q,o}_{(j-1)} \left(\frac{Z_{3(j-1)+3}}{Z^q_{(j-1)}} \right).
\end{aligned} \tag{A.4}$$

Thus, the growth rates of the proxy series are used to generate monthly consumption data for quarter q. Summing over the quarter yields

$$\tilde{C}^{q,o}_{(j)} = \sum_{m=1}^{3} \tilde{C}^o_{3(j-1)+m} = C^{q,o}_{(j-1)} \left[\frac{Z_{3(j-1)+1}}{Z^q_{(j-1)}} + \frac{Z_{3(j-1)+2}}{Z^q_{(j-1)}} + \frac{Z_{3(j-1)+3}}{Z^q_{(j-1)}} \right] = C^{q,o}_{(j-1)} \frac{Z^q_{(j)}}{Z^q_{(j-1)}}. \tag{A.5}$$

In Step 2, we adjust the monthly estimates $\tilde{C}^o_{3(j-1)+m}$ by the factor $C^{q,o}_{(j)}/\tilde{C}^{q,o}_{(j)}$, which leads to

$$\begin{aligned} C^o_{3(j-1)+1} &= \tilde{C}^o_{3(j-1)+1}\left(\frac{C^{q,o}_{(j)}}{\tilde{C}^{q,o}_{(j)}}\right) = C^{q,o}_{(j)}\frac{Z_{3(j-1)+1}}{Z^q_{(j)}} \\ C^o_{3(j-1)+2} &= \tilde{C}^o_{3(j-1)+2}\left(\frac{C^{q,o}_{(j)}}{\tilde{C}^{q,o}_{(j)}}\right) = C^{q,o}_{(j)}\frac{Z_{3(j-1)+2}}{Z^q_{(j)}} \\ C^o_{3(j-1)+3} &= \tilde{C}^o_{3(j-1)+3}\left(\frac{C^{q,o}_{(j)}}{\tilde{C}^{q,o}_{(j)}}\right) = C^{q,o}_{(j)}\frac{Z_{3(j-1)+3}}{Z^q_{(j)}} \end{aligned} \tag{A.6}$$

and guarantees that

$$C^{q,o}_{(j)} = \sum_{m=1}^{3} C^o_{3(j-1)+m}.$$

We now define the growth rates $g^o_{c,t} = \log C^o_t - \log C^o_{t-1}$ and $g_{c,t} = \log C_t - \log C_{t-1}$. By taking logarithmic transformations of (A.3) and (A.6) and combining the resulting equations, we can deduce that the growth rates for the second and third month of quarter q are given by

$$\begin{aligned} g^o_{c,3(j-1)+2} &= g_{c,3(j-1)+2} + \epsilon_{3(j-1)+2} - \epsilon_{3(j-1)+1} \\ g^o_{c,3(j-1)+3} &= g_{c,3(j-1)+3} + \epsilon_{3(j-1)+3} - \epsilon_{3(j-1)+2}. \end{aligned} \tag{A.7}$$

The derivation of the growth rate between the third month of quarter $j-1$ and the first month of quarter j is a bit more cumbersome. Using (A.6), we can write the growth rate as

$$\begin{aligned} g^o_{c,3(j-1)+1} &= \log C^{q,o}_{(j)} + \log Z_{3(j-1)+1} - \log Z^q_{(j)} \\ &\quad - \log C^{q,o}_{(j-1)} - \log Z_{3(j-2)+3} + \log Z^q_{(j-1)}. \end{aligned} \tag{A.8}$$

To simplify (A.8) further, we are using a log-linear approximation. Suppose we log-linearize an equation of the form

$$X^q_{(j)} = X_{3(j-1)+1} + X_{3(j-1)+2} + X_{3(j-1)+3}$$

around X^q_* and $X_* = X^q_*/3$, using lowercase variables to denote percentage deviations from the log-linearization point. Then,

$$x^q_{(j)} \approx \frac{1}{3}(x_{3(j-1)+1} + x_{3(j-1)+2} + x_{3(j-1)+3}).$$

Using (A.3) and the definition of quarterly variables as sums of monthly variables, we can apply the log-linearization as follows:

$$\log C^{q,o}_{(j)} - \log Z^q_{(j)} = \log(C^q_*/Z^q_*) + \epsilon^q_{(j)} - \frac{1}{3}\big(\epsilon_{3(j-1)+1} + \epsilon_{3(j-1)+2} + \epsilon_{3(j-1)+3}\big). \tag{A.9}$$

Substituting (A.9) into (A.8) yields

$$\begin{aligned} g^o_{c,3(j-1)+1} &= g_{c,3(j-1)+1} + \epsilon_{3(j-1)+1} - \epsilon_{3(j-2)+3} + \epsilon^q_{(j)} - \epsilon^q_{(j-1)} \\ &\quad -\frac{1}{3}\big(\epsilon_{3(j-1)+1} + \epsilon_{3(j-1)+2} + \epsilon_{3(j-1)+3}\big) + \frac{1}{3}\big(\epsilon_{3(j-2)+1} + \epsilon_{3(j-2)+2} + \epsilon_{3(j-2)+3}\big). \end{aligned} \tag{A.10}$$

An "annual" version of this equation appears in the main text.

C Solving the Long-Run Risks Model

This section provides solutions for the consumption and dividend claims for the endowment process:

$$\begin{aligned}
g_{c,t+1} &= \mu_c + x_t + \sigma_{c,t}\eta_{c,t+1} \\
g_{d,t+1} &= \mu_d + \phi x_t + \pi\sigma_{c,t}\eta_{c,t+1} + \sigma_{d,t}\eta_{d,t+1} \\
x_{t+1} &= \rho x_t + \sigma_{x,t}\eta_{x,t+1} \\
x_{\lambda,t+1} &= \rho_\lambda x_{\lambda,t} + \sigma_\lambda \eta_{\lambda,t+1} \\
\sigma^2_{c,t+1} &= (1-\nu_c)(\varphi_c\bar{\sigma})^2 + \nu_c\sigma^2_{c,t} + \sigma_{w_c} w_{c,t+1} \\
\sigma^2_{x,t+1} &= (1-\nu_x)(\varphi_x\bar{\sigma})^2 + \nu_x\sigma^2_{x,t} + \sigma_{w_x} w_{x,t+1} \\
\sigma^2_{d,t+1} &= (1-\nu_d)(\varphi_d\bar{\sigma})^2 + \nu_d\sigma^2_{d,t} + \sigma_{w_d} w_{d,t+1} \\
&\quad \eta_{i,t+1}, \eta_{\lambda,t+1}, w_{i,t+1} \sim N(0,1), \quad i \in \{c,x,d\}.
\end{aligned} \tag{A.11}$$

The Euler equation for the economy is

$$\mathbb{E}_t\left[\exp\left(m_{t+1} + r_{i,t+1}\right)\right] = 1, \quad i \in \{c,m\}, \tag{A.12}$$

where

$$m_{t+1} = \theta \log\delta + \theta x_{\lambda,t+1} - \frac{\theta}{\psi} g_{c,t+1} + (\theta-1) r_{c,t+1} \tag{A.13}$$

is the log of the real stochastic discount factor (SDF), $r_{c,t+1}$ is the log return on the consumption claim, and $r_{m,t+1}$ is the log market return. (A.13) is derived in Section C.6 below. Returns are given by the approximation of Campbell and Shiller (1988a):

$$\begin{aligned}
r_{c,t+1} &= \kappa_0 + \kappa_1 pc_{t+1} - pc_t + g_{c,t+1} \\
r_{m,t+1} &= \kappa_{0,m} + \kappa_{1,m} pd_{t+1} - pd_t + g_{d,t+1}.
\end{aligned} \tag{A.14}$$

The risk premium on any asset is

$$\mathbb{E}_t(r_{i,t+1} - r_{f,t}) + \frac{1}{2} Var_t(r_{i,t+1}) = -Cov_t(m_{t+1}, r_{i,t+1}). \tag{A.15}$$

In Section C.1 we solve for the law of motion for the return on the consumption claim, $r_{c,t+1}$. In Section C.2 we solve for the law of motion for the market return, $r_{m,t+1}$. The risk-free rate is derived in Section C.3. All three solutions depend on linearization parameters that are derived in Section C.4. Finally, as mentioned above, the SDF is derived in Section C.6.

C.1 Consumption Claim

In order to derive the dynamics of asset prices, we rely on approximate analytical solutions. Specifically, we conjecture that the price-consumption ratio follows

$$pc_t = A_0 + A_1 x_t + A_{1,\lambda} x_{\lambda,t} + A_{2,c}\sigma_{c,t}^2 + A_{2,x}\sigma_{x,t}^2 \tag{A.16}$$

and solve for A's using (A.11), (A.12), (A.14), and (A.16).

From (A.11), (A.14), and (A.16)

$$\begin{aligned} r_{c,t+1} &= \left\{\kappa_0 + A_0(\kappa_1 - 1) + \mu_c + \kappa_1 A_{2,x}(1-\nu_x)(\varphi_x\bar{\sigma})^2 + \kappa_1 A_{2,c}(1-\nu_c)(\varphi_c\bar{\sigma})^2\right\} \\ &+ \frac{1}{\psi}x_t + A_{1,\lambda}(\kappa_1\rho_\lambda - 1)x_{\lambda,t} + A_{2,x}(\kappa_1\nu_x - 1)\sigma_{x,t}^2 + A_{2,c}(\kappa_1\nu_c - 1)\sigma_{c,t}^2 \\ &+ \sigma_{c,t}\eta_{c,t+1} + \kappa_1 A_1\sigma_{x,t}\eta_{x,t+1} + \kappa_1 A_{1,\lambda}\sigma_\lambda\eta_{\lambda,t+1} + \kappa_1 A_{2,x}\sigma_{w_x}w_{x,t+1} + \kappa_1 A_{2,c}\sigma_{w_c}w_{c,t+1} \end{aligned} \tag{A.17}$$

and from (A.11), (A.12), (A.14), and (A.16)

$$\begin{aligned} m_{t+1} &= (\theta-1)\left\{\kappa_0 + A_0(\kappa_1 - 1) + \kappa_1 A_{2,x}(1-\nu_x)(\varphi_x\bar{\sigma})^2 + \kappa_1 A_{2,c}(1-\nu_c)(\varphi_c\bar{\sigma})^2\right\} \\ &- \gamma\mu + \theta\log\delta - \frac{1}{\psi}x_t + \rho_\lambda x_{\lambda,t} + (\theta-1)A_{2,x}(\kappa_1\nu_x - 1)\sigma_{x,t}^2 + (\theta-1)A_{2,c}(\kappa_1\nu_c - 1)\sigma_{c,t}^2 \\ &- \gamma\sigma_{c,t}\eta_{c,t+1} + (\theta-1)\kappa_1 A_1\sigma_{x,t}\eta_{x,t+1} + \left\{(\theta-1)\kappa_1 A_{1,\lambda} + \theta\right\}\sigma_\lambda\eta_{\lambda,t+1} \\ &+ (\theta-1)\kappa_1 A_{2,x}\sigma_{w_x}w_{x,t+1} + (\theta-1)\kappa_1 A_{2,c}\sigma_{w_c}w_{c,t+1}. \end{aligned} \tag{A.18}$$

The solutions for A's that describe the dynamics of the price-consumption ratio are determined from

$$\mathbb{E}_t\left[m_{t+1} + r_{c,t+1}\right] + \frac{1}{2}Var_t\left[m_{t+1} + r_{c,t+1}\right] = 0$$

and they are

$$A_1 = \frac{1 - \frac{1}{\psi}}{1 - \kappa_1\rho}, \quad A_{1,\lambda} = \frac{\rho_\lambda}{1 - \kappa_1\rho_\lambda}, \quad A_{2,x} = \frac{\frac{\theta}{2}(\kappa_1 A_1)^2}{1 - \kappa_1\nu_x}, \quad A_{2,c} = \frac{\frac{\theta}{2}(1 - \frac{1}{\psi})^2}{1 - \kappa_1\nu_c} \tag{A.19}$$

and $A_0 = \frac{A_0^1 + A_0^2}{1-\kappa_1}$, where

$$\begin{aligned} A_0^1 &= \log\delta + \kappa_0 + \mu(1 - \frac{1}{\psi}) + \kappa_1 A_{2,x}(1-\nu_x)(\varphi_x\bar{\sigma})^2 + \kappa_1 A_{2,c}(1-\nu_c)(\varphi_c\bar{\sigma})^2 \\ A_0^2 &= \frac{\theta}{2}\left\{(\kappa_1 A_{1,\lambda} + 1)^2\sigma_\lambda^2 + (\kappa_1 A_{2,x}\sigma_{w_x})^2 + (\kappa_1 A_{2,c}\sigma_{w_c})^2\right\}. \end{aligned}$$

For convenience, (A.18) can be rewritten as

$$m_{t+1} - \mathbb{E}_t[m_{t+1}] = \lambda_c\sigma_{c,t}\eta_{c,t+1} + \lambda_x\sigma_{x,t}\eta_{x,t+1} + \lambda_\lambda\sigma_\lambda\eta_{\lambda,t+1} + \lambda_{w_x}\sigma_{w_x}w_{x,t+1} + \lambda_{w_c}\sigma_{w_c}w_{c,t+1}.$$

Note that λs represent the market price of risk for each source of risk. To be specific,

$$\begin{aligned}\lambda_c &= -\gamma, \quad \lambda_x = -(\gamma - \frac{1}{\psi})\frac{\kappa_1}{1-\kappa_1\rho}, \quad \lambda_\lambda = \frac{\theta - \kappa_1\rho_\lambda}{1-\kappa_1\rho_\lambda}, \\ \lambda_{w_x} &= -\frac{\theta(\gamma-\frac{1}{\psi})(1-\frac{1}{\psi})\kappa_1}{2(1-\kappa_1\nu_x)}(\frac{\kappa_1}{1-\kappa_1\rho})^2, \quad \lambda_{w_c} = -\frac{\theta(\gamma-\frac{1}{\psi})(1-\frac{1}{\psi})\kappa_1}{2(1-\kappa_1\nu_c)}.\end{aligned} \tag{A.20}$$

Similarly, rewrite (A.17) as

$$r_{c,t+1} - \mathbb{E}_t[r_{c,t+1}] = -\beta_{c,c}\sigma_{c,t}\eta_{c,t+1} - \beta_{c,x}\sigma_{x,t}\eta_{x,t+1} - \beta_{c,\lambda}\sigma_\lambda\eta_{\lambda,t+1} - \beta_{c,w_x}\sigma_{w_x}w_{x,t+1} - \beta_{c,w_c}\sigma_{w_c}w_{c,t+1}$$

where

$$\beta_{c,c} = -1, \quad \beta_{c,x} = -\kappa_1 A_1, \quad \beta_{c,\lambda} = -\kappa_1 A_{1,\lambda}, \quad \beta_{c,w_x} = -\kappa_1 A_{2,x}, \quad \beta_{c,w_c} = -\kappa_1 A_{2,c}. \tag{A.21}$$

The risk premium for the consumption claim is

$$\begin{aligned}\mathbb{E}_t(r_{c,t+1} - r_{f,t}) + \frac{1}{2}Var_t(r_{c,t+1}) &= -Cov_t(m_{t+1}, r_{c,t+1}) \\ &= \beta_{c,x}\lambda_x\sigma^2_{x,t} + \beta_{c,c}\lambda_c\sigma^2_{c,t} + \beta_{c,\lambda}\lambda_\lambda\sigma^2_\lambda + \beta_{c,w_x}\lambda_{w_x}\sigma^2_{w_x} + \beta_{c,w_c}\lambda_{w_c}\sigma^2_{w_c}.\end{aligned} \tag{A.22}$$

C.2 Market Return

Similarly, using the conjectured solution to the price-dividend ratio

$$pd_t = A_{0,m} + A_{1,m}x_t + A_{1,\lambda,m}x_{\lambda,t} + A_{2,x,m}\sigma^2_{x,t} + A_{2,c,m}\sigma^2_{c,t} + A_{2,d,m}\sigma^2_{d,t} \tag{A.23}$$

the market return can be expressed as

$$\begin{aligned}r_{m,t+1} &= \kappa_{0,m} + A_{0,m}(\kappa_{1,m}-1) + \mu_d + \kappa_{1,m}A_{2,x,m}(1-\nu_x)(\varphi_x\bar{\sigma})^2 \\ &+ \kappa_{1,m}A_{2,c,m}(1-\nu_c)(\varphi_c\bar{\sigma})^2 + \kappa_{1,m}A_{2,d,m}(1-\nu_d)(\varphi_d\bar{\sigma})^2 + \{\phi + A_{1,m}(\kappa_{1,m}\rho - 1)\}x_t \\ &+ (\kappa_{1,m}\rho_\lambda - 1)A_{1,\lambda,m}x_{\lambda,t} + A_{2,x,m}(\kappa_{1,m}\nu_x - 1)\sigma^2_{x,t} + A_{2,c,m}(\kappa_{1,m}\nu_c - 1)\sigma^2_{c,t} \\ &+ A_{2,d,m}(\kappa_{1,m}\nu_d - 1)\sigma^2_{d,t} + \pi\sigma_{c,t}\eta_{c,t+1} + \sigma_{d,t}\eta_{d,t+1} + \kappa_{1,m}A_{1,m}\sigma_{x,t}\eta_{x,t+1} + \kappa_{1,m}A_{1,\lambda,m}\sigma_\lambda\eta_{\lambda,t+1} \\ &+ \kappa_{1,m}A_{2,x,m}\sigma_{w_x}w_{x,t+1} + \kappa_{1,m}A_{2,c,m}\sigma_{w_c}w_{c,t+1} + \kappa_{1,m}A_{2,d,m}\sigma_{w_d}w_{d,t+1}.\end{aligned} \tag{A.24}$$

Given the solution for A's, A_m's can be derived as follows:

$$\begin{aligned}
A_{0,m} &= \frac{A_{0,m}^{1st} + A_{0,m}^{2nd}}{1-\kappa_{1,m}} \\
A_{1,m} &= \frac{\phi - \frac{1}{\psi}}{1-\kappa_{1,m}\rho} \\
A_{1,\lambda,m} &= \frac{\rho_\lambda}{1-\kappa_{1,m}\rho_\lambda} \\
A_{2,x,m} &= \frac{\frac{1}{2}\left\{(\theta-1)\kappa_1 A_1 + \kappa_{1,m}A_{1,m}\right\}^2 + (\theta-1)(\kappa_1\nu_x - 1)A_{2,x}}{1-\kappa_{1,m}\nu_x} \\
A_{2,c,m} &= \frac{\frac{1}{2}(\pi-\gamma)^2 + (\theta-1)(\kappa_1\nu_c - 1)A_{2,c}}{1-\kappa_{1,m}\nu_c} \\
A_{2,d,m} &= \frac{\frac{1}{2}}{1-\kappa_{1,m}\nu_d},
\end{aligned} \tag{A.25}$$

where

$$\begin{aligned}
A_{0,m}^{1st} &= \theta\log\delta + (\theta-1)\left\{\kappa_0 + A_0(\kappa_1-1) + \kappa_1 A_{2,x}(1-\nu_x)(\varphi_x\bar{\sigma})^2 + \kappa_1 A_{2,c}(1-\nu_c)(\varphi_c\bar{\sigma})^2\right\} \\
&- \gamma\mu + \kappa_{0,m} + \mu_d + \kappa_{1,m}A_{2,x,m}(1-\nu_x)(\varphi_x\bar{\sigma})^2 + \kappa_{1,m}A_{2,c,m}(1-\nu_c)(\varphi_c\bar{\sigma})^2 \\
&+ \kappa_{1,m}A_{2,d,m}(1-\nu_d)(\varphi_d\bar{\sigma})^2 \\
A_{0,m}^{2nd} &= \frac{1}{2}\left(\kappa_{1,m}A_{2,x,m}\sigma_{w_x} + (\theta-1)\kappa_1 A_{2,x}\sigma_{w_x}\right)^2 + \frac{1}{2}\left(\kappa_{1,m}A_{2,c,m}\sigma_{w_c} + (\theta-1)\kappa_1 A_{2,c}\sigma_{w_c}\right)^2 \\
&+ \frac{1}{2}\left(\kappa_{1,m}A_{2,d,m}\sigma_{w_d}\right)^2 + \frac{1}{2}\left(\kappa_{1,m}A_{1,\lambda,m}\sigma_\lambda + (\theta-1)\kappa_1 A_{1,\lambda}\sigma_\lambda + \theta\sigma_\lambda\right)^2.
\end{aligned}$$

Rewrite market-return equation (A.24) as

$$r_{m,t+1} - \mathbb{E}_t[r_{m,t+1}] = -\beta_{m,c}\sigma_{c,t}\eta_{c,t+1} - \beta_{m,x}\sigma_{x,t}\eta_{x,t+1} - \beta_{m,\lambda}\sigma_\lambda\eta_{\lambda,t+1} - \beta_{m,w_x}\sigma_{w_x}w_{x,t+1} - \beta_{m,w_c}\sigma_{w_c}w_{c,t+1},$$

where

$$\begin{aligned}
\beta_{m,c} &= -\pi, \quad \beta_{m,x} = -\kappa_{1,m}A_{1,m}, \quad \beta_{m,\lambda} = -\kappa_{1,m}A_{1,\lambda,m}, \\
\beta_{m,w_x} &= -\kappa_{1,m}A_{2,x,m}, \quad \beta_{m,w_c} = -\kappa_{1,m}A_{2,c,m}.
\end{aligned} \tag{A.26}$$

The risk premium for the dividend claim is

$$\begin{aligned}
E_t(r_{m,t+1} - r_{f,t}) + \frac{1}{2}Var_t(r_{m,t+1}) &= -Cov_t(m_{t+1}, r_{m,t+1}) \\
&= \beta_{m,x}\lambda_x\sigma_{x,t}^2 + \beta_{m,c}\lambda_c\sigma_{c,t}^2 + \beta_{m,\lambda}\lambda_\lambda\sigma_\lambda^2 + \beta_{m,w_x}\lambda_{w_x}\sigma_{w_x}^2 + \beta_{m,w_c}\lambda_{w_c}\sigma_{w_c}^2.
\end{aligned} \tag{A.27}$$

C.3 Risk-Free Rate

The model-driven equation for the risk-free rate is

$$\begin{aligned} r_{f,t} &= -\mathbb{E}_t\left[m_{t+1}\right] - \frac{1}{2}Var_t\left[m_{t+1}\right] \\ &= -\theta\log\delta - \mathbb{E}_t\left[x_{\lambda,t+1}\right] + \frac{\theta}{\psi}\mathbb{E}_t\left[g_{c,t+1}\right] + (1-\theta)\mathbb{E}_t\left[r_{c,t+1}\right] - \frac{1}{2}Var_t\left[m_{t+1}\right]. \end{aligned} \tag{A.28}$$

Subtract $(1-\theta)r_{f,t}$ from both sides and divide by θ,

$$r_{f,t} = -\log\delta - \frac{1}{\theta}\mathbb{E}_t\left[x_{\lambda,t+1}\right] + \frac{1}{\psi}\mathbb{E}_t\left[g_{c,t+1}\right] + \frac{(1-\theta)}{\theta}\mathbb{E}_t\left[r_{c,t+1} - r_{f,t}\right] - \frac{1}{2\theta}Var_t\left[m_{t+1}\right] \tag{A.29}$$

From (A.11) and (A.18)

$$r_{f,t} = B_0 + B_1 x_t + B_{1,\lambda}x_{\lambda,t} + B_{2,x}\sigma^2_{x,t} + B_{2,c}\sigma^2_{c,t},$$

where

$$B_1 = \frac{1}{\psi}, \quad B_{1,\lambda} = -\rho_\lambda, \quad B_{2,x} = -\frac{(1-\frac{1}{\psi})(\gamma-\frac{1}{\psi})\kappa_1^2}{2(1-\kappa_1\rho)^2}, \quad B_{2,c} = -\frac{1}{2}(\frac{\gamma-1}{\psi}+\gamma) \tag{A.30}$$

and

$$\begin{aligned} B_0 &= -\theta\log\delta - (\theta-1)\left\{\kappa_0 + (\kappa_1-1)A_0 + \kappa_1 A_{2,x}(1-\nu_x)(\varphi_x\bar{\sigma})^2 + \kappa_1 A_{2,c}(1-\nu_c)(\varphi_c\bar{\sigma})^2\right\} \\ &+ \gamma\mu - \frac{1}{2}\left\{(\theta-1)\kappa_1 A_{2,x}\sigma_{w_x}\right\}^2 - \frac{1}{2}\left\{(\theta-1)\kappa_1 A_{2,c}\sigma_{w_c}\right\}^2 - \frac{1}{2}\left\{((\theta-1)\kappa_1 A_{1,\lambda}+\theta)^2\sigma^2_\lambda\right\}. \end{aligned}$$

C.4 Linearization Parameters

For any asset, the linearization parameters are determined endogenously by the following system of equations:

$$\begin{aligned} \bar{pd}_i &= A_{0,i}(\bar{pd}_i) + \sum_{j\in\{c,x,d\}} A_{2,i,j}(\bar{pd}_i)\times(\varphi_j\bar{\sigma})^2 \\ \kappa_{1,i} &= \frac{\exp(\bar{pd}_i)}{1+\exp(\bar{pd}_i)} \\ \kappa_{0,i} &= \log(1+\exp(\bar{pd}_i)) - \kappa_{1,i}\bar{pd}_i. \end{aligned}$$

The solution is determined numerically by iteration until reaching a fixed point of $\bar{pd}_i$.

C.5 Zero-Coupon Real Bonds

Let $p_{n,t}$ be the log t-price of an n-period zero-coupon real bond. Conjecture that $p_{n,t}$ is a linear function of state variables

$$p_{n,t} = C_{n,0} + C_{n,1}x_t + C_{n,1\lambda}x_{\lambda,t} + C_{n,2x}\sigma^2_{x,t} + C_{n,2c}\sigma^2_{c,t}. \tag{A.31}$$

The pricing equation implies

$$p_{n,t} = \mathbb{E}_t\left[p_{n-1,t+1} + m_{t+1}\right] + \frac{1}{2}Var_t\left[p_{n-1,t+1} + m_{t+1}\right]. \tag{A.32}$$

The coefficients of the pricing equation are expressed recursively as

$$\begin{aligned}
C_{n,1} &= C_{n-1,1}\rho - \frac{1}{\psi} \qquad (A.33)\\
C_{n,1\lambda} &= C_{n-1,1\lambda}\rho_\lambda + \rho_\lambda\\
C_{n,2x} &= C_{n-1,2x}\nu_x + (\theta-1)A_{2,x}(\kappa_1\nu_x - 1) + \frac{1}{2}\left\{C_{n-1,1} + (\theta-1)\kappa_1 A_1\right\}^2\\
C_{n,2c} &= C_{n-1,2c}\nu_c + (\theta-1)A_{2,c}(\kappa_1\nu_c - 1) + \frac{1}{2}\gamma^2\\
C_{n,0} &= \theta\log\delta + (\theta-1)\left\{\kappa_0 + (\kappa_1-1)A_0 + \kappa_1 A_{2,x}(1-\nu_x)(\varphi_x\bar{\sigma})^2 + \kappa_1 A_{2,c}(1-\nu_c)(\varphi_c\bar{\sigma})^2\right\}\\
&\quad -\gamma\mu + C_{n-1,0} + C_{n-1,2x}(1-\nu_x)(\varphi_x\bar{\sigma})^2 + C_{n-1,2c}(1-\nu_c)(\varphi_c\bar{\sigma})^2\\
&\quad +\frac{1}{2}\left(C_{n-1,1\lambda} + \left\{(\theta-1)\kappa_1 A_{1,\lambda} + \theta\right\}\right)^2\sigma^2_\lambda + \frac{1}{2}\left((\theta-1)\kappa_1 A_{2,x} + C_{n-1,2x}\right)^2\sigma^2_{w_x}\\
&\quad +\frac{1}{2}\left((\theta-1)\kappa_1 A_{2,c} + C_{n-1,2c}\right)^2\sigma^2_{w_c}
\end{aligned}$$

with initial conditions that $C_{0,1} = C_{0,1\lambda} = C_{0,2x} = C_{0,2c} = C_{0,0} = 0$. However, in order to develop economic intuition, it is useful to express them in a non-recursive fashion:

$$\begin{aligned}
C_{n,1} &= -\frac{1}{\psi}\frac{(1-\rho^n)}{(1-\rho)}, \quad n \geq 1\\
C_{n,1\lambda} &= \rho_\lambda\frac{(1-\rho_\lambda^n)}{(1-\rho_\lambda)}, \quad n \geq 1\\
C_{n,2x} &= \left((\theta-1)A_{2,x}(\kappa_1\nu_x - 1) + \frac{1}{2}\left\{-\frac{1}{\psi}\frac{(1-\rho^{n-1})}{(1-\rho)} + (\theta-1)\kappa_1 A_1\right\}^2\right)\frac{(1-\nu_x^n)}{(1-\nu_x)}, \quad n \geq 2\\
C_{n,2c} &= \left((\theta-1)A_{2,c}(\kappa_1\nu_c - 1) + \frac{1}{2}\gamma^2\right)\frac{(1-\nu_c^n)}{(1-\nu_c)}, \quad n \geq 1.
\end{aligned}$$

Define return on an n-period zero-coupon bond as

$$r_{n,t+1} = p_{n-1,t+1} - p_{n,t}.$$

The risk premium for the bond return is

$$\begin{aligned} & E_t(r_{n,t+1} - r_{f,t}) + \frac{1}{2} Var_t(r_{n,t+1}) \qquad (A.34) \\ = \; & -cov_t(m_{t+1}, r_{n,t+1}) \\ = \; & -(\theta-1)\kappa_1 A_{2,c} C_{n-1,2c} \sigma_{w_c}^2 - (\theta-1)\kappa_1 A_{2,x} C_{n-1,2x} \sigma_{w_x}^2 - \{(\theta-1)\kappa_1 A_{1,\lambda} + \theta\} C_{n-1,1\lambda} \sigma_\lambda^2 \\ & -(\theta-1)\kappa_1 A_1 C_{n-1,1} \sigma_{x,t}^2. \end{aligned}$$

C.6 Deriving the Intertemporal Marginal Rate of Substitution (MRS)

We consider a representative-agent endowment economy modified to allow for time-preference shocks. The representative agent has Epstein and Zin (1989) recursive preferences and maximizes her lifetime utility

$$V_t = \max_{C_t} \left[(1-\delta)\lambda_t C_t^{\frac{1-\gamma}{\theta}} + \delta \big(\mathbb{E}_t [V_{t+1}^{1-\gamma}] \big)^{\frac{1}{\theta}} \right]^{\frac{\theta}{1-\gamma}}$$

subject to budget constraint

$$W_{t+1} = (W_t - C_t) R_{c,t+1},$$

where W_t is the wealth of the agent, $R_{c,t+1}$ is the return on all invested wealth, γ is risk aversion, $\theta = \frac{1-\gamma}{1-1/\psi}$, and ψ is intertemporal elasticity of substitution. The ratio $\frac{\lambda_{t+1}}{\lambda_t}$ determines how agents trade off current versus future utility and is referred to as the time-preference shock (see Albuquerque, Eichenbaum, Luo, and Rebelo (2016)).

First conjecture a solution for $V_t = \phi_t W_t$. The value function is homogenous of degree 1 in wealth; it can now be written as

$$\phi_t W_t = \max_{C_t} \left[(1-\delta)\lambda_t C_t^{\frac{1-\gamma}{\theta}} + \delta \big(\mathbb{E}_t [(\phi_{t+1} W_{t+1})^{1-\gamma}] \big)^{\frac{1}{\theta}} \right]^{\frac{\theta}{1-\gamma}} \qquad (A.35)$$

subject to

$$W_{t+1} = (W_t - C_t) R_{c,t+1}.$$

Epstein and Zin (1989) show that the above dynamic program has a maximum.

Using the dynamics of the wealth equation, we substitute W_{t+1} into (A.35) to derive

$$\phi_t W_t = \max_{C_t} \left[(1-\delta)\lambda_t C_t^{\frac{1-\gamma}{\theta}} + \delta (W_t - C_t)^{\frac{1-\gamma}{\theta}} \big(\mathbb{E}_t [(\phi_{t+1} R_{c,t+1})^{1-\gamma}] \big)^{\frac{1}{\theta}} \right]^{\frac{\theta}{1-\gamma}}. \qquad (A.36)$$

At the optimum, $C_t = b_t W_t$, where b_t is the consumption-wealth ratio. Using (A.36) and shifting the exponent on the braces to the left-hand side, and dividing by W_t, yields

$$\phi_t^{\frac{1-\gamma}{\theta}} = (1-\delta)\lambda_t \left(\frac{C_t}{W_t} \right)^{\frac{1-\gamma}{\theta}} + \delta \left(1 - \frac{C_t}{W_t} \right)^{\frac{1-\gamma}{\theta}} \big(\mathbb{E}_t [(\phi_{t+1} R_{c,t+1})^{1-\gamma}] \big)^{\frac{1}{\theta}} \qquad (A.37)$$

or simply

$$\phi_t^{\frac{1-\gamma}{\theta}} = (1-\delta)\lambda_t b_t^{\frac{1-\gamma}{\theta}} + \delta(1-b_t)^{\frac{1-\gamma}{\theta}}\left(\mathbb{E}_t[(\phi_{t+1}R_{c,t+1})^{1-\gamma}]\right)^{\frac{1}{\theta}}. \tag{A.38}$$

The first-order condition with respect to the consumption choice yields

$$(1-\delta)\lambda_t b_t^{\frac{1-\gamma}{\theta}-1} = \delta(1-b_t)^{\frac{1-\gamma}{\theta}-1}\left(\mathbb{E}_t[(\phi_{t+1}R_{c,t+1})^{1-\gamma}]\right)^{\frac{1}{\theta}}. \tag{A.39}$$

Plugging (A.39) into (A.38) yields

$$\phi_t = (1-\delta)^{\frac{\theta}{1-\gamma}}\lambda_t^{\frac{\theta}{1-\gamma}}\left(\frac{C_t}{W_t}\right)^{\frac{1-\gamma-\theta}{1-\gamma}} = (1-\delta)^{\frac{\psi}{\psi-1}}\lambda_t^{\frac{\psi}{\psi-1}}\left(\frac{C_t}{W_t}\right)^{\frac{1}{1-\psi}}. \tag{A.40}$$

The lifetime value function is $\phi_t W_t$, with the solution to ϕ_t stated above. This expression for ϕ_t is important: It states that the maximized lifetime utility is determined by the consumption-wealth ratio.

(A.39) can be rewritten as

$$(1-\delta)^{\theta}\lambda_t^{\theta}\left(\frac{b_t}{1-b_t}\right)^{-\frac{\theta}{\psi}} = \delta^{\theta}\mathbb{E}_t[(\phi_{t+1}R_{c,t+1})^{1-\gamma}]. \tag{A.41}$$

Consider the term $\phi_{t+1}R_{c,t+1}$:

$$\phi_{t+1}R_{c,t+1} = (1-\delta)^{\frac{\psi}{\psi-1}}\lambda_{t+1}^{\frac{\psi}{\psi-1}}\left(\frac{C_{t+1}}{W_{t+1}}\right)^{\frac{1}{1-\psi}}R_{c,t+1}. \tag{A.42}$$

After substituting the wealth constraint, $\frac{C_{t+1}}{W_{t+1}} = \frac{C_{t+1}/C_t}{W_t/C_t - 1}\cdot\frac{1}{R_{c,t+1}} = \frac{G_{t+1}}{R_{c,t+1}}\cdot\frac{b_t}{1-b_t}$, into the above expression, it follows that

$$\phi_{t+1}R_{c,t+1} = (1-\delta)^{\frac{\psi}{\psi-1}}\lambda_{t+1}^{\frac{\psi}{\psi-1}}\left(\frac{b_t}{1-b_t}\right)^{\frac{1}{1-\psi}}\left(\frac{G_{t+1}}{R_{c,t+1}}\right)^{\frac{1}{1-\psi}}R_{c,t+1}. \tag{A.43}$$

After some intermediate tedious manipulations,

$$\delta^{\theta}(\phi_{t+1}R_{c,t+1})^{1-\gamma} = \delta^{\theta}(1-\delta)^{\theta}\lambda_{t+1}^{\theta}\left(\frac{b_t}{1-b_t}\right)^{-\frac{\theta}{\psi}}G_{t+1}^{-\frac{\theta}{\psi}}R_{c,t+1}^{\theta}. \tag{A.44}$$

Taking expectations and substituting the last expression into (A.41) yields

$$\delta^{\theta}\mathbb{E}_t[\left(\frac{\lambda_{t+1}}{\lambda_t}\right)^{\theta}G_{t+1}^{-\frac{\theta}{\psi}}R_{c,t+1}^{\theta-1}R_{c,t+1}] = 1. \tag{A.45}$$

From here we see that the MRS in terms of observables is

$$M_{t+1} = \delta^{\theta}\left(\frac{\lambda_{t+1}}{\lambda_t}\right)^{\theta}G_{t+1}^{-\frac{\theta}{\psi}}R_{c,t+1}^{\theta-1}. \tag{A.46}$$

The log of MRS is

$$m_{t+1} = \theta\log\delta + \theta x_{\lambda,t+1} - \frac{\theta}{\psi}g_{t+1} + (\theta-1)r_{c,t+1}, \tag{A.47}$$

where $x_{\lambda,t+1} = \log(\frac{\lambda_{t+1}}{\lambda_t})$.

D The State-Space Representation of the LRR Model

Below we describe the the state-space representation for the LRR model. The state-space representation for the cash-flow-only specifications can be obtained by eliminating the asset returns ($r_{m,t+1}$ and $r_{f,t}$) from the set of measurement equations.

D.1 Measurement Equations

In order to capture the correlation structure between the measurement errors at monthly frequency, we assumed in the main text that 12 months of consumption growth data are released at the end of each year. We will now present the resulting measurement equation. To simplify the exposition, we assume that the monthly consumption data are released at the end of the quarter (rather than at the end of the year). In the main text, the measurement equation is written as

$$y_{t+1} = A_{t+1}\Big(D + Zs_{t+1} + Z^v s^v_{t+1}(h_{t+1}, h_t) + \Sigma^u u_{t+1}\Big), \quad u_{t+1} \sim N(0, I). \tag{A.48}$$

The selection matrix A_{t+1} accounts for the deterministic changes in the vector of observables, y_{t+1}. Recall that monthly observations are available only starting in 1959:M1. For the sake of exposition, suppose prior to 1959:M1 consumption growth was available at quarterly frequency. We further assume that dividend growth data are always available in the form of time-aggregated quarterly data. Then (we are omitting some of the o superscripts for observed series that we used in the main text):

1. Prior to 1959:M1:

   (a) If $t+1$ is the last month of the quarter:

$$y_{t+1} = \begin{bmatrix} g^q_{c,t+1} \\ g^q_{d,t+1} \\ r_{m,t+1} \\ r_{f,t} \end{bmatrix}, \quad A_{t+1} = \begin{bmatrix} \frac{1}{3} & \frac{2}{3} & 1 & \frac{2}{3} & \frac{1}{3} & 0 & 0 & 0 \\ 0 & 0 & 0 & 0 & 0 & 1 & 0 & 0 \\ 0 & 0 & 0 & 0 & 0 & 0 & 1 & 0 \\ 0 & 0 & 0 & 0 & 0 & 0 & 0 & 1 \end{bmatrix}.$$

   (b) If $t+1$ is not the last month of the quarter:

$$y_{t+1} = \begin{bmatrix} g^q_{d,t+1} \\ r_{m,t+1} \\ r_{f,t} \end{bmatrix}, \quad A_{t+1} = \begin{bmatrix} 0 & 0 & 0 & 0 & 0 & 1 & 0 & 0 \\ 0 & 0 & 0 & 0 & 0 & 0 & 1 & 0 \\ 0 & 0 & 0 & 0 & 0 & 0 & 0 & 1 \end{bmatrix}.$$

2. From 1959:M1 to present:

(a) If $t+1$ is the last month of the quarter:

$$y_{t+1} = \begin{bmatrix} g_{c,t+1} \\ g_{c,t} \\ g_{c,t-1} \\ g^q_{d,t+1} \\ r_{m,t+1} \\ r_{f,t} \end{bmatrix}, \quad A_{t+1} = \begin{bmatrix} 1 & 0 & 0 & 0 & 0 & 0 & 0 & 0 \\ 0 & 1 & 0 & 0 & 0 & 0 & 0 & 0 \\ 0 & 0 & 1 & 0 & 0 & 0 & 0 & 0 \\ 0 & 0 & 0 & 0 & 0 & 1 & 0 & 0 \\ 0 & 0 & 0 & 0 & 0 & 0 & 1 & 0 \\ 0 & 0 & 0 & 0 & 0 & 0 & 0 & 1 \end{bmatrix}$$

(b) If $t+1$ is not the last month of the quarter:

$$y_{t+1} = \begin{bmatrix} g^q_{d,t+1} \\ r_{m,t+1} \\ r_{f,t} \end{bmatrix}, \quad A_{t+1} = \begin{bmatrix} 0 & 0 & 0 & 0 & 0 & 1 & 0 & 0 \\ 0 & 0 & 0 & 0 & 0 & 0 & 1 & 0 \\ 0 & 0 & 0 & 0 & 0 & 0 & 0 & 1 \end{bmatrix}.$$

The relationship between observations and states (ignoring the measurement errors) is given by the approximate analytical solution of the LRR model described in Section C:

$$\begin{aligned} g_{c,t+1} &= \mu_c + x_t + \sigma_{c,t}\eta_{c,t+1} \\ g_{d,t+1} &= \mu_d + \phi x_t + \pi\sigma_{c,t}\eta_{c,t+1} + \sigma_{d,t}\eta_{d,t+1} \\ r_{m,t+1} &= \{\kappa_{0,m} + (\kappa_{1,m}-1)A_{0,m} + \mu_d\} \\ &+ (\kappa_{1,m}A_{1,m})x_{t+1} + (\phi - A_{1,m})x_t + (\kappa_{1,m}A_{1,\lambda,m})x_{\lambda,t+1} - A_{1,\lambda,m}x_{\lambda,t} + \pi\sigma_{c,t}\eta_{c,t+1} + \sigma_{d,t}\eta_{d,t+1} \\ &+ (\kappa_{1,m}A_{2,x,m})\sigma^2_{x,t+1} - A_{2,x,m}\sigma^2_{x,t} + (\kappa_{1,m}A_{2,c,m})\sigma^2_{c,t+1} - A_{2,c,m}\sigma^2_{c,t} + (\kappa_{1,m}A_{2,d,m})\sigma^2_{d,t+1} - A_{2,d,m}\sigma^2_{d,t} \\ r_{f,t} &= B_0 + B_1 x_t + B_{1,\lambda}x_{\lambda,t} + B_{2,x}\sigma^2_{x,t} + B_{2,c}\sigma^2_{c,t} \\ &\eta_{i,t+1}, \eta_{\lambda,t+1}, w_{i,t+1} \sim N(0,1), \quad i \in \{c,x,d\}. \end{aligned} \tag{A.49}$$

In order to reproduce (A.49) and the measurement-error structure described in Sections 2.1 and 2.2, we define the vectors of states s_{t+1} and s^v_{t+1} as

$$s_{t+1} = \begin{bmatrix} x_{t+1} \\ x_t \\ x_{t-1} \\ x_{t-2} \\ x_{t-3} \\ x_{t-4} \\ \sigma_{c,t}\eta_{c,t+1} \\ \sigma_{c,t-1}\eta_{c,t} \\ \sigma_{c,t-2}\eta_{c,t-1} \\ \sigma_{c,t-3}\eta_{c,t-2} \\ \sigma_{c,t-4}\eta_{c,t-3} \\ \sigma_{\epsilon}\epsilon_{t+1} \\ \sigma_{\epsilon}\epsilon_{t} \\ \sigma_{\epsilon}\epsilon_{t-1} \\ \sigma_{\epsilon}\epsilon_{t-2} \\ \sigma_{\epsilon}\epsilon_{t-3} \\ \sigma_{\epsilon}\epsilon_{t-4} \\ \sigma^q_{\epsilon}\epsilon^q_{t+1} \\ \sigma^q_{\epsilon}\epsilon^q_{t} \\ \sigma^q_{\epsilon}\epsilon^q_{t-1} \\ \sigma^q_{\epsilon}\epsilon^q_{t-2} \\ \sigma_{d,t}\eta_{d,t+1} \\ \sigma_{d,t-1}\eta_{d,t} \\ \sigma_{d,t-2}\eta_{d,t-1} \\ \sigma_{d,t-3}\eta_{d,t-2} \\ \sigma_{d,t-4}\eta_{d,t-3} \\ x_{\lambda,t+1} \\ x_{\lambda,t} \end{bmatrix}, \quad s^v_{t+1} = \begin{bmatrix} \sigma^2_{x,t+1} \\ \sigma^2_{x,t} \\ \sigma^2_{c,t+1} \\ \sigma^2_{c,t} \\ \sigma^2_{d,t+1} \\ \sigma^2_{d,t} \end{bmatrix}. \tag{A.50}$$

It can be verified that the coefficient matrices D, Z, Z^v, and Σ^e are given by

$$Z = \left[\begin{array}{cccccccccccccccccccccccccccc}
0 & 1 & 0 & 0 & 0 & 0 & 1 & 0 & 0 & 0 & 0 & 1 & -1 & 0 & 0 & 0 & 0 & 0 & 0 & 0 & 0 & 0 & 0 & 0 & 0 & 0 & 0 & 0 \\
0 & 0 & 1 & 0 & 0 & 0 & 0 & 1 & 0 & 0 & 0 & 0 & 1 & -1 & 0 & 0 & 0 & 0 & 0 & 0 & 0 & 0 & 0 & 0 & 0 & 0 & 0 & 0 \\
0 & 0 & 0 & 1 & 0 & 0 & 0 & 0 & 1 & 0 & 0 & -\frac{1}{3} & -\frac{1}{3} & \frac{2}{3} & -\frac{2}{3} & \frac{1}{3} & \frac{1}{3} & 1 & 0 & 0 & -1 & 0 & 0 & 0 & 0 & 0 & 0 & 0 \\
0 & 0 & 0 & 0 & 1 & 0 & 0 & 0 & 0 & 1 & 0 & 0 & 0 & 0 & 1 & -1 & 0 & 0 & 0 & 0 & 0 & 0 & 0 & 0 & 0 & 0 & 0 & 0 \\
0 & 0 & 0 & 0 & 0 & 1 & 0 & 0 & 0 & 0 & 1 & 0 & 0 & 0 & 0 & 1 & -1 & 0 & 0 & 0 & 0 & 0 & 0 & 0 & 0 & 0 & 0 & 0 \\
0 & \frac{\phi}{3} & \frac{2\phi}{3} & \phi & \frac{2\phi}{3} & \frac{\phi}{3} & \frac{\pi}{3} & \frac{2\pi}{3} & \pi & \frac{2\pi}{3} & \frac{\pi}{3} & 0 & 0 & 0 & 0 & 0 & 0 & 0 & 0 & 0 & 0 & \frac{1}{3} & \frac{2}{3} & 1 & \frac{2}{3} & \frac{1}{3} & 0 & 0 \\
\mu_{r,1} & \mu_{r,2} & 0 & 0 & 0 & 0 & \mu_{r,3} & 0 & 0 & 0 & 0 & 0 & 0 & 0 & 0 & 0 & 0 & 0 & 0 & 0 & 0 & \mu_{r,4} & 0 & 0 & 0 & 0 & \mu_{r,5} & \mu_{r,6} \\
0 & B_1 & 0 & 0 & 0 & 0 & 0 & 0 & 0 & 0 & 0 & 0 & 0 & 0 & 0 & 0 & 0 & 0 & 0 & 0 & 0 & 0 & 0 & 0 & 0 & 0 & B_{1,\lambda} & 0
\end{array}\right]$$

$$Z^v = \left[\begin{array}{cccccc}
0 & 0 & 0 & 0 & 0 & 0 \\
0 & 0 & 0 & 0 & 0 & 0 \\
0 & 0 & 0 & 0 & 0 & 0 \\
0 & 0 & 0 & 0 & 0 & 0 \\
0 & 0 & 0 & 0 & 0 & 0 \\
0 & 0 & 0 & 0 & 0 & 0 \\
\mu_{r,7} & \mu_{r,8} & \mu_{r,9} & \mu_{r,10} & \mu_{r,11} & \mu_{r,12} \\
0 & B_{2,x} & 0 & B_{2,c} & 0 & 0
\end{array}\right], \quad D = \left[\begin{array}{c} \mu \\ \mu \\ \mu \\ \mu \\ \mu \\ 3\mu_d \\ \mu_{r,0} \\ B_0 \end{array}\right], \quad \Sigma^u = \left[\begin{array}{cccccccc}
0 & 0 & 0 & 0 & 0 & 0 & 0 & 0 \\
0 & 0 & 0 & 0 & 0 & 0 & 0 & 0 \\
0 & 0 & 0 & 0 & 0 & 0 & 0 & 0 \\
0 & 0 & 0 & 0 & 0 & 0 & 0 & 0 \\
0 & 0 & 0 & 0 & 0 & 0 & 0 & 0 \\
0 & 0 & 0 & 0 & 0 & \sigma^a_{d,\epsilon} & 0 & 0 \\
0 & 0 & 0 & 0 & 0 & 0 & 0 & 0 \\
0 & 0 & 0 & 0 & 0 & 0 & 0 & \sigma_{f,\epsilon}
\end{array}\right].$$

The coefficients $\mu_{r,0}$ to $\mu_{r,12}$ are obtained from the solution of the LRR model:

$$\begin{bmatrix} \mu_{r,0} \\ \mu_{r,1} \\ \mu_{r,2} \\ \mu_{r,3} \\ \mu_{r,4} \\ \mu_{r,5} \\ \mu_{r,6} \end{bmatrix} = \begin{bmatrix} \kappa_{0,m} + A_{0,m}(\kappa_{1,m} - 1) + \mu_d \\ \kappa_{1,m} A_{1,m} \\ \phi - A_{1,m} \\ \pi \\ 1 \\ \kappa_{1,m} A_{1,\lambda,m} \\ -A_{1,\lambda,m} \end{bmatrix}, \quad \begin{bmatrix} \mu_{r,7} \\ \mu_{r,8} \\ \mu_{r,9} \\ \mu_{r,10} \\ \mu_{r,11} \\ \mu_{r,12} \end{bmatrix} = \begin{bmatrix} \kappa_{1,m} A_{2,x,m} \\ -A_{2,x,m} \\ \kappa_{1,m} A_{2,c,m} \\ -A_{2,c,m} \\ \kappa_{1,m} A_{2,d,m} \\ -A_{2,d,m} \end{bmatrix}.$$

D.2 State Transition Equations

Using the definition of s_{t+1} in (A.50), we write the state-transition equation as

$$s_{t+1} = \Phi s_t + v_{t+1}(h_t). \tag{A.51}$$

Conditional on the volatilities h_t, this equation reproduces the law of motion of the two persistent conditional mean processes

$$\begin{aligned} x_{t+1} &= \rho x_t + \sigma_{x,t}\eta_{x,t+1} \\ x_{\lambda,t+1} &= \rho_\lambda x_{\lambda,t} + \sigma_\lambda \eta_{\lambda,t+1} \end{aligned} \tag{A.52}$$

and it contains some trivial relationships among the measurement-error states. The matrices Φ and $v_{t+1}(h_t)$ are defined as

$$\Phi = \begin{bmatrix}
\rho & 0 & 0 & 0 & 0 & 0 & 0 & 0 & 0 & 0 & 0 & 0 & 0 & 0 & 0 & 0 & 0 & 0 & 0 & 0 & 0 & 0 & 0 & 0 & 0 & 0 & 0 \\
1 & 0 & 0 & 0 & 0 & 0 & 0 & 0 & 0 & 0 & 0 & 0 & 0 & 0 & 0 & 0 & 0 & 0 & 0 & 0 & 0 & 0 & 0 & 0 & 0 & 0 & 0 \\
0 & 1 & 0 & 0 & 0 & 0 & 0 & 0 & 0 & 0 & 0 & 0 & 0 & 0 & 0 & 0 & 0 & 0 & 0 & 0 & 0 & 0 & 0 & 0 & 0 & 0 & 0 \\
0 & 0 & 1 & 0 & 0 & 0 & 0 & 0 & 0 & 0 & 0 & 0 & 0 & 0 & 0 & 0 & 0 & 0 & 0 & 0 & 0 & 0 & 0 & 0 & 0 & 0 & 0 \\
0 & 0 & 0 & 1 & 0 & 0 & 0 & 0 & 0 & 0 & 0 & 0 & 0 & 0 & 0 & 0 & 0 & 0 & 0 & 0 & 0 & 0 & 0 & 0 & 0 & 0 & 0 \\
0 & 0 & 0 & 0 & 1 & 0 & 0 & 0 & 0 & 0 & 0 & 0 & 0 & 0 & 0 & 0 & 0 & 0 & 0 & 0 & 0 & 0 & 0 & 0 & 0 & 0 & 0 \\
0 & 0 & 0 & 0 & 0 & 0 & 0 & 0 & 0 & 0 & 0 & 0 & 0 & 0 & 0 & 0 & 0 & 0 & 0 & 0 & 0 & 0 & 0 & 0 & 0 & 0 & 0 \\
0 & 0 & 0 & 0 & 0 & 0 & 1 & 0 & 0 & 0 & 0 & 0 & 0 & 0 & 0 & 0 & 0 & 0 & 0 & 0 & 0 & 0 & 0 & 0 & 0 & 0 & 0 \\
0 & 0 & 0 & 0 & 0 & 0 & 0 & 1 & 0 & 0 & 0 & 0 & 0 & 0 & 0 & 0 & 0 & 0 & 0 & 0 & 0 & 0 & 0 & 0 & 0 & 0 & 0 \\
0 & 0 & 0 & 0 & 0 & 0 & 0 & 0 & 1 & 0 & 0 & 0 & 0 & 0 & 0 & 0 & 0 & 0 & 0 & 0 & 0 & 0 & 0 & 0 & 0 & 0 & 0 \\
0 & 0 & 0 & 0 & 0 & 0 & 0 & 0 & 0 & 1 & 0 & 0 & 0 & 0 & 0 & 0 & 0 & 0 & 0 & 0 & 0 & 0 & 0 & 0 & 0 & 0 & 0 \\
0 & 0 & 0 & 0 & 0 & 0 & 0 & 0 & 0 & 0 & 0 & 0 & 0 & 0 & 0 & 0 & 0 & 0 & 0 & 0 & 0 & 0 & 0 & 0 & 0 & 0 & 0 \\
0 & 0 & 0 & 0 & 0 & 0 & 0 & 0 & 0 & 0 & 0 & 0 & 1 & 0 & 0 & 0 & 0 & 0 & 0 & 0 & 0 & 0 & 0 & 0 & 0 & 0 & 0 \\
0 & 0 & 0 & 0 & 0 & 0 & 0 & 0 & 0 & 0 & 0 & 0 & 0 & 1 & 0 & 0 & 0 & 0 & 0 & 0 & 0 & 0 & 0 & 0 & 0 & 0 & 0 \\
0 & 0 & 0 & 0 & 0 & 0 & 0 & 0 & 0 & 0 & 0 & 0 & 0 & 0 & 1 & 0 & 0 & 0 & 0 & 0 & 0 & 0 & 0 & 0 & 0 & 0 & 0 \\
0 & 0 & 0 & 0 & 0 & 0 & 0 & 0 & 0 & 0 & 0 & 0 & 0 & 0 & 0 & 1 & 0 & 0 & 0 & 0 & 0 & 0 & 0 & 0 & 0 & 0 & 0 \\
0 & 0 & 0 & 0 & 0 & 0 & 0 & 0 & 0 & 0 & 0 & 0 & 0 & 0 & 0 & 0 & 1 & 0 & 0 & 0 & 0 & 0 & 0 & 0 & 0 & 0 & 0 \\
0 & 0 & 0 & 0 & 0 & 0 & 0 & 0 & 0 & 0 & 0 & 0 & 0 & 0 & 0 & 0 & 0 & 1 & 0 & 0 & 0 & 0 & 0 & 0 & 0 & 0 & 0 \\
0 & 0 & 0 & 0 & 0 & 0 & 0 & 0 & 0 & 0 & 0 & 0 & 0 & 0 & 0 & 0 & 0 & 0 & 1 & 0 & 0 & 0 & 0 & 0 & 0 & 0 & 0 \\
0 & 0 & 0 & 0 & 0 & 0 & 0 & 0 & 0 & 0 & 0 & 0 & 0 & 0 & 0 & 0 & 0 & 0 & 0 & 1 & 0 & 0 & 0 & 0 & 0 & 0 & 0 \\
0 & 0 & 0 & 0 & 0 & 0 & 0 & 0 & 0 & 0 & 0 & 0 & 0 & 0 & 0 & 0 & 0 & 0 & 0 & 0 & 1 & 0 & 0 & 0 & 0 & 0 & 0 \\
0 & 0 & 0 & 0 & 0 & 0 & 0 & 0 & 0 & 0 & 0 & 0 & 0 & 0 & 0 & 0 & 0 & 0 & 0 & 0 & 0 & 1 & 0 & 0 & 0 & 0 & 0 \\
0 & 0 & 0 & 0 & 0 & 0 & 0 & 0 & 0 & 0 & 0 & 0 & 0 & 0 & 0 & 0 & 0 & 0 & 0 & 0 & 0 & 0 & 1 & 0 & 0 & 0 & 0 \\
0 & 0 & 0 & 0 & 0 & 0 & 0 & 0 & 0 & 0 & 0 & 0 & 0 & 0 & 0 & 0 & 0 & 0 & 0 & 0 & 0 & 0 & 0 & 1 & 0 & 0 & 0 \\
0 & 0 & 0 & 0 & 0 & 0 & 0 & 0 & 0 & 0 & 0 & 0 & 0 & 0 & 0 & 0 & 0 & 0 & 0 & 0 & 0 & 0 & 0 & 0 & \rho_\lambda & 0 \\
0 & 0 & 0 & 0 & 0 & 0 & 0 & 0 & 0 & 0 & 0 & 0 & 0 & 0 & 0 & 0 & 0 & 0 & 0 & 0 & 0 & 0 & 0 & 0 & 1 & 0
\end{bmatrix}$$

and

$$v_{t+1}(h_t) = \begin{bmatrix} \sigma_{x,t}\eta_{x,t+1} \\ 0 \\ 0 \\ 0 \\ 0 \\ 0 \\ \sigma_{c,t}\eta_{c,t+1} \\ 0 \\ 0 \\ 0 \\ 0 \\ \sigma_\epsilon \epsilon_{t+1} \\ 0 \\ 0 \\ 0 \\ 0 \\ 0 \\ \sigma_\epsilon^q \epsilon_{t+1}^q \\ 0 \\ 0 \\ 0 \\ \sigma_{d,t}\eta_{d,t+1} \\ 0 \\ 0 \\ 0 \\ 0 \\ \sigma_\lambda \eta_{\lambda,t+1} \\ 0 \end{bmatrix}.$$

The law of motion of the three persistent conditional log volatility processes is given by

$$h_{t+1} = \Psi h_t + \Sigma_h w_{t+1}, \tag{A.53}$$

where

$$h_{t+1} = \begin{bmatrix} h_{x,t+1} \\ h_{c,t+1} \\ h_{d,t+1} \end{bmatrix}, \quad \Psi = \begin{bmatrix} \rho_{h_x} & 0 & 0 \\ 0 & \rho_{h_c} & 0 \\ 0 & 0 & \rho_{h_d} \end{bmatrix}$$

$$\Sigma_h = \begin{bmatrix} \sigma_{h_x}\sqrt{1-\rho_{h_x}^2} & 0 & 0 \\ 0 & \sigma_{h_c}\sqrt{1-\rho_{h_c}^2} & 0 \\ 0 & 0 & \sigma_{h_d}\sqrt{1-\rho_{h_d}^2} \end{bmatrix}, \quad w_{t+1} = \begin{bmatrix} w_{x,t+1} \\ w_{c,t+1} \\ w_{d,t+1} \end{bmatrix}.$$

We express

$$\sigma_{x,t} = \varphi_x \sigma \exp(h_{x,t}), \quad \sigma_{c,t} = \varphi_c \sigma \exp(h_{c,t}), \quad \sigma_{d,t} = \varphi_d \sigma \exp(h_{d,t}),$$

which delivers the dependence on h_t in the above definition of $v_{t+1}(\cdot)$. $\varphi_c = 1$ is normalized.

Table A-1: Prior Distributions

	Consumption					Dividend			
	Distr.	5%	50%	95%		Distr.	5%	50%	95%
μ_c	N	-.007	.0016	.0100	μ_c	N	-.007	.0016	.0100
ρ	U	-.90	0	.90	ϕ	U	.50	5.0	9.50
φ_x	U	.05	.50	.95	φ_d	U	.50	5.0	9.50
σ	IG	.0008	.0019	.0061	π	U	.50	5.0	9.50
ρ_{h_c}	N^T	.27	.80	.999	ρ_{h_d}	N^T	.27	.80	.999
$\sigma^2_{h_c}$	IG	.0011	.0060	.0283	$\sigma^2_{h_d}$	IG	.015	.0445	.208
σ_ϵ	IG	.0008	.0019	.0061	$\frac{\sigma^a_{d,\epsilon}}{\sigma(g_d^{a,o})}$	U	.05	.50	.95
σ^a_ϵ	IG	.0007	.0029	.0386					

Notes: N, N^T, G, IG, and U denote normal, truncated (outside of the interval $(-1,1)$) normal, gamma, inverse gamma, and uniform distributions, respectively.

E Posterior Inference

The prior distribution used for the empirical analysis in this paper is summarized in Table A-1. To construct a posterior sampler for the LRR model, we use a particle-filter approximation of the likelihood function, constructed as follows. Our state-space representation, given the measurement equation (A.48) and the state transition equations (A.51) and (A.53). Note that conditional on the volatility is linear conditional on the volatility states (h_{t+1}, h_t). The particle filter uses a swarm of particles $\{z_t^j, W_t^j\}_{j=1}^M$ to approximate

$$\mathbb{E}[h(z_t)|Y_{1:t}] \approx \frac{1}{M}\sum_{j=1}^{M} W_t^j h(z_t^j). \tag{A.54}$$

Throughout this section we omit the parameter vector Θ from the conditioning set. Here $h(\cdot)$ is an integrable function of z_t and the approximation $\approx$, under suitable regularity conditions, can be stated formally in terms of a strong law of large numbers and a central limit theorem. In general, z_t^j would be composed of h_t^j, h_{t-1}^j, and s_t^j. However, given that the state-space model is linear conditional on (h_t, h_{t-1}), we can replace s_t^j by

$$\left[vec\big(\mathbb{E}[s_t|h_t^j, h_{t-1}^j, Y_{1:t}]\big),\ vech\big(Var[s_t|h_t^j, h_{t-1}^j, Y_{1:t}]\big)\right]',$$

where $vech(\cdot)$ stacks the non-redundant elements of a symmetric matrix. The use of the vector of conditional means and covariance terms for s_t in the definition of the particle z_t^j leads to a vari-

ance reduction in the particle filter approximation of the likelihood function. The implementation of the particle filter is based on Algorithm 13 in Herbst and Schorfheide (2015). The particle-filter approximation of the likelihood function is embedded into a fairly standard random walk Metropolis-Hastings algorithm (see Chapter 9 of Herbst and Schorfheide (2015)).